energies

MDPI

Article

An Improved Ångström-Type Model for Estimating Solar Radiation over the Tibetan Plateau

Jiandong Liu [1,2], Tao Pan [3,4,*], Deliang Chen [2], Xiuji Zhou [1], Qiang Yu [5], Gerald N. Flerchinger [6], De Li Liu [7], Xintong Zou [3,8], Hans W. Linderholm [2], Jun Du [9], Dingrong Wu [1] and Yanbo Shen [10]

1 State Key Laboratory of Severe Weather, Chinese Academy of Meteorological Sciences, Beijing 100081, China; liujd2001@263.net (J.L.); xjzhou@cams.cma.gov.cn (X.Z.); wudr@cams.cma.gov.cn (D.W.)
2 Regional Climate Group, Department of Earth Sciences, University of Gothenburg, SE-405 30 Gothenburg, Sweden; deliang@gvc.gu.se (D.C.); hansl@gvc.gu.se (H.W.L.)
3 Key Laboratory of Land Surface Pattern and Simulation, Institute of Geographic Sciences and Natural Resources Research, Chinese Academy of Sciences, Beijing 100101, China; zouxt.15s@igsnrr.ac.cn
4 Center for System Integration and Sustainability, Michigan State University, East Lansing, MI 48823, USA
5 Plant Functional and Climate Change Cluster, University of Technology, Sydney 2007, Australia; uts.edu.au@gmail.com
6 USDA-ARS, Northwest Watershed Research Center, Boise, ID 83712, USA; gerald.flerchinger@ars.usda.gov
7 NSW Department of Primary Industries, Wagga Wagga Agricultural Institute, PMB, Wagga Wagga, NSW 2650, Australia; de.li.liu@dpi.nsw.gov.au
8 University of Chinese Academy of Sciences, Beijing 100049, China
9 Climate Center, Tibet Autonomous Meteorological Administration, Lhasa 850000, China; dujun0891@163.com
10 Centre for Solar and Wind Energy Research, China Meteorological Administration, Beijing 100081, China; shenyb@cma.gov.cn
* Correspondence: pantao@igsnrr.ac.cn; Tel.: +86-10-6488-9692; Fax: +86-10-6485-1844

Academic Editor: Tariq Al-Shemmeri
Received: 3 May 2017; Accepted: 23 June 2017; Published: 1 July 2017

Abstract: For estimating the annual mean of daily solar irradiation in plateau mountainous regions, observed data from 15 radiation stations were used to validate different empirical estimation methods over the Tibetan Plateau. Calibration indicates that sunshine-based site-dependent models perform better than temperature-based ones. Then, the highly rated sunshine-based Ångström model and temperature-based Bristow model were selected for regional application. The geographical models perform much better than the average models, but still not ideally. To achieve better performance, the Ångström-type model was improved using altitude and water vapor pressure as the leading factors. The improved model can accurately predict the coefficients at all the stations, and performs the best among all models with an average *Nash-Sutcliffe Efficiency* value of 0.856. Spatial distribution of the annual mean of daily solar irradiation was then estimated with the improved model. It is indicated that there is an increasing trend of radiation from east to west, with a great center of the annual mean of daily solar irradiation on southwest Tibetan Plateau ranging from 20 to 24 MJ·m^{-2}. The improved model should be further validated against observations before its applications in other plateau mountainous regions.

Keywords: improved Ångström-type model; solar radiation estimation; Tibetan Plateau

1. Introduction

Solar radiation plays a critical role in most land surface processes including physical, biological and chemical processes, e.g., hydrological cycling, vegetation growth, climate and weather change [1–4].

It is also one of the key input variables in crop growth, and hydrological and climate models [5–9]. However, unlike other meteorological elements such as temperature and precipitation, solar radiation is observed only at very few stations due to scarcity of instruments and high cost of maintenance [5,10]. Thus, estimation of solar radiation becomes an indispensable method for energy harvest and model application.

Several methods are available for solar radiation estimation including numerical models, artificial neutral networks, satellites measurements, etc. Some complex dynamic numerical models were established based on meteorological theory for the relationships between solar radiation and other meteorological variables, including aerosol concentrations [11,12]. This kind of model usually requires many input variables that can hardly be applied practically. Solar radiation can also be estimated by artificial neutral network [13–17] and satellite-based remote sensing methods [18–20]. However, training neutral network usually requires large datasets and the resulting model may not be applicable to other regions [10]. The low sampling frequency resulting from cloudiness and the coarse spatial resolution always make satellite-based remote sensing methods inadequate for site-specific application [21]. In addition, there is no satellite-based database covering the Tibetan Plateau (TP) except the National Aeronautics and Space Administration-Surface meteorology and Solar Energy (NASA-SSE) product and several commercially-available products by companies. The NASA-SSE is free, but is currently limited to 1983 to 2005 [22]. In contrast to the models mentioned above, several simple empirical models have been developed and widely used as the primary tools for solar radiation estimation. These are typically based on the relationship between solar radiation and readily available meteorological variables, such as sunshine hours [23–27], temperature [28–33], and precipitation [34,35]. Many previous studies have established that the sunshine-based models always outperform other types of models [30,36–39].

Requirements of empirical models are relatively easy to meet, and the models themselves are easy to apply. However, the necessity to calibrate empirical models indicates that their coefficients are changing with locations, e.g., [9,30,34,37,40–42]. The site-dependent coefficients restrict regional application of the empirical models, which is a big challenge for spatial rasterization. To solve this problem, the model coefficients for regional application were obtained by simply averaging coefficients at different locations [43], or fitting coefficients from an overall regional database combining all of the datasets at different locations [44]. In the view of statistical theory [45], both of these two methods have the same premise that the variation in coefficients should be small between different locations, which seems to be supported by previous reports made in the plain regions [42,44]. However, up to now, this assumption has never been tested thoroughly under complex terrain conditions. Recently, some geographic models were also developed for regional applications [46–50] by means of fitting the coefficients with geographical information such as latitude, longitude and altitude. Although these models perform quite well in the plain regions, they have not been tested thoroughly under complex terrain conditions like the TP. Thus, integrated comparison and evaluation of different ways of determining regional coefficients of the empirical models are needed for future applications in the complex terrains conditions, like the Tibetan Plateau.

Located in Southwest China and known as the Third Pole, the TP is the highest contiguous region in the world, and has abundant solar energy resources because of its high elevation [51]. However, up to now, few research studies on solar radiation estimation over the TP have been made, compared to the numerous reports on the plain regions, e.g., [30,34,36,37,42]. Pan et al. [52] proposed a method to rasterize daily global solar radiation over the TP based on the diurnal temperature ranges with the Bristow-Campbell model, but the Bristow-Campbell model is a temperature-based model, which is thought to be inferior to the sunshine-based ones [30,36–39]. Li et al. [53] evaluated the performance of eight sunshine-based models on the TP, and proposed two average models for estimating solar radiation on the TP, based on fitting coefficients to the composite database involving all selected stations. However, the coefficients of the sunshine-based models reflect the transmission characteristics of the atmosphere at its calibration site [42], which is determined by the optical path of the sunlight affected by the altitude [54], we can reasonably hypothesize that coefficients of the sunshine-based models would vary greatly due to great variation of the altitude under complex terrain conditions, meaning that the models suggested by Li et al. [53] can only be used to estimate solar radiation at certain locations on the TP. Thus, an innovative sunshine-based model has to be developed for more accurate estimation of the distribution of solar radiation under complex terrain conditions on the TP.

In this study, the annual mean of daily solar irradiation from 15 solar stations on the TP and its surrounding regions were collected and analyzed. The objectives of this research are: (1) to thoroughly test the hypothesis that the coefficients of the empirical models vary considerably on the TP and its adjacent areas; (2) to compare the performances of different methods on determining regional coefficients of the empirical models over the TP; and (3) to identify the leading factors accounting for the variations in coefficients and develop an innovative simple sunshine-type model for accurate estimation of the distribution of the annual mean of solar irradiation over the TP.

2. Results

2.1. Spatial and Temporal Pattern of Observed Annual Mean of Solar Irradiation

The fifteen radiation stations were classified into six groups according to altitude, and the variations of the annual mean of daily solar irradiation from 1993 to 2010 for each group can be seen in Figure 1. Generally speaking, temporal variations are relatively stable at all stations except an abrupt drop around 2008 at Panzhihua. There is a general trend that the annual mean of daily solar irradiation becomes greater with increasing altitude. The annual mean of daily solar irradiation on the TP, such as at Lhasa, Shiquanhe and Naqu, is much greater than that in its surrounding regions like Panzhihua. The lowest annual mean of daily solar irradiation occurs in Ermeishan with a value of 13.35 MJ·m^{-2}, due to large cloud coverage. The greatest annual mean of solar irradiation occurs at Shiquanhe, with a value of 21.49 MJ·m^{-2}. Greater annual mean of daily irradiation on the TP again validates the assumption that abundant solar energy resources are held on the TP due to its higher elevation [38,51]. These data are fundamental supports for the validation of estimated spatial radiation distribution on the TP.

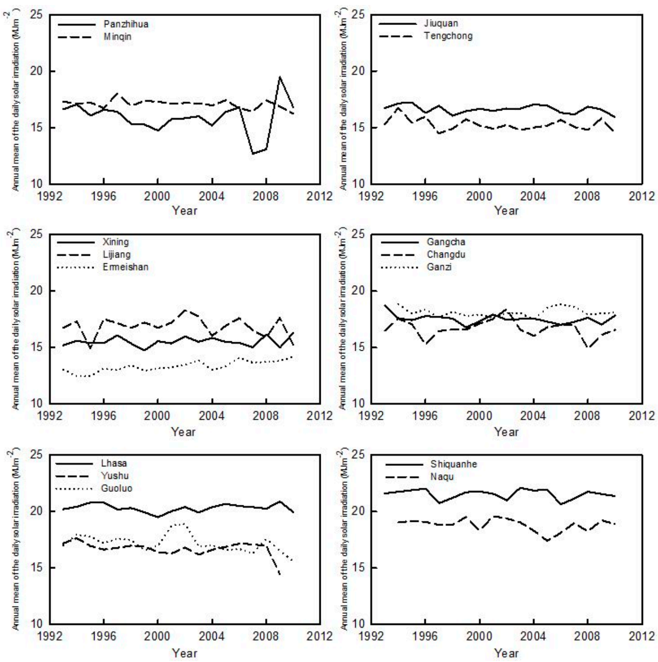

Figure 1. Variation of annual mean of daily solar irradiation on the Tibetan Plateau and its surrounding regions.

2.2. Comparison of the Performances of Different Methods on Estimation of Daily Solar Irradiation

The coefficients of site-dependent models were first fitted for each of the selected 15 stations. Each pair of the coefficients of *a* and *b* relates to the corresponding station, meaning that these coefficients cannot be used in the regional scale. However, based on these coefficients, regional coefficients are obtained by average, geographical, and modeling methods as follows.

2.2.1. Site-Dependent Models

First, the three sunshine-based models, Ångström, Ogelman and Bahell, were calibrated with the datasets from 1993 to 2007 (Table 1). Coefficients of *a* and *b* in the Ångström model range from 0.173 in Panzhihua to 0.291 in Ganzi, and from 0.498 in Panzhihua to 0.603 in Changdu, respectively. Similar variations can also be found in the coefficients of Ogelman and Bahell models. Though the coefficients are different for different stations, the average values of *NSE* of the three sunshine-based models are nearly the same, with values of 0.885, 0.886 and 0.887 respectively. The other evaluation indicators such as *MAPE*, *RRMSE*, *Slope* and *Inter* also confirm the similar model performance. The three temperature-based models were then calibrated at each station using the same period of data (Table 1). The coefficients of *a*, *b* and *c* in Bristow model also vary considerably, ranging from 0.601 in Panzhihua to 1.005 in Changdu, from 0.005 in Gangcha to 0.057 in Tengchong, and from 1.18 in Tengchong to 2.340 in Gangcha, respectively. Similar variations in the coefficients can also be found in the calibration results of the Hargreaves and Chen models. The *NSE* values of the three temperature-based models are also quite similar, with average values of 0.672, 0.671 and 0.673, respectively. Compared with the sunshine-based models, the *NSE* values of the three temperature-based models are much lower, indicating sunshine-based models have obvious advantages over the temperature-based ones in model calibration on the TP.

Table 1. Calibration of the sunshine- and temperature-based site-dependent models at different locations using data from 1993 to 2007 in this study.

Sunshine-Based Models	Station	*a*	*b*	*c*	*d*	*NSE*	*MAPE*	*RRMSE*	*Slope*	*Inter*	*n*
Angstrom	Jiuquan	0.219	0.514	-	-	0.948	8.629	10.004	0.901	1.547	5469
	Minqin	0.193	0.541	-	-	0.951	7.647	9.333	0.930	1.161	5466
	Gangcha	0.198	0.603	-	-	0.915	8.530	11.022	0.941	1.129	5430
	Xining	0.215	0.530	-	-	0.936	9.681	11.301	0.904	1.463	5458
	Shiquanhe	0.229	0.616	-	-	0.856	8.138	11.448	0.890	2.578	5433
	Naqu	0.271	0.574	-	-	0.818	9.706	13.095	0.897	2.103	5294
	Lhasa	0.283	0.530	-	-	0.885	6.856	8.958	0.883	2.371	5283
	Yushu	0.229	0.560	-	-	0.913	9.103	10.837	0.919	1.397	5473
	Guoluo	0.247	0.563	-	-	0.888	9.506	12.107	0.917	1.546	5456
	Changdu	0.218	0.592	-	-	0.871	9.386	11.828	0.883	1.973	5468
	Ganzi	0.291	0.511	-	-	0.884	8.630	11.070	0.872	2.318	5068
	Ermeishan	0.234	0.565	-	-	0.826	18.275	21.327	0.887	1.659	5472
	Lijiang	0.222	0.538	-	-	0.891	9.991	11.303	0.870	2.170	5440
	Panzhihua	0.173	0.498	-	-	0.883	11.287	13.218	0.857	2.201	5475
	Tengchong	0.215	0.506	-	-	0.810	13.127	15.534	0.827	2.648	5471
	Average	0.229	0.549	-	-	0.885	9.899	12.159	0.892	1.184	5410

Table 1. *Cont.*

Sunshine-Based Models	**Station**	***a***	***b***	***c***	***d***	***NSE***	***MAPE***	***RRMSE***	***Slope***	***Inter***	***n***
Ogelman	Jiuquan	0.227	0.468	0.044	-	0.948	8.541	10.010	0.900	1.562	5469
	Minqin	0.203	0.482	0.056	-	0.951	7.619	9.333	0.929	1.196	5466
	Gangcha	0.199	0.596	0.007	-	0.915	8.527	11.022	0.941	1.132	5430
	Xining	0.203	0.628	−0.110	-	0.938	9.709	11.115	0.906	1.423	5458
	Shiquanhe	0.271	0.459	0.124	-	0.856	8.168	11.421	0.888	2.641	5433
	Naqu	0.286	0.504	0.064	-	0.818	9.682	13.091	0.894	2.175	5294
	Lhasa	0.272	0.575	−0.038	-	0.885	6.841	8.949	0.887	2.309	5283
	Yushu	0.255	0.423	0.137	-	0.914	8.980	10.741	0.924	1.315	5473
	Guoluo	0.261	0.475	0.088	-	0.888	9.502	12.071	0.912	1.630	5456
	Changdu	0.255	0.386	0.217	-	0.874	9.219	11.689	0.878	2.067	5468
	Ganzi	0.281	0.568	−0.057	-	0.885	8.635	11.028	0.876	2.240	5068
	Ermeishan	0.234	0.574	−0.010	-	0.826	18.277	21.351	0.888	1.664	5472
	Lijiang	0.217	0.573	−0.035	-	0.892	10.059	11.275	0.875	2.098	5440
	Panzhihua	0.167	0.544	−0.048	-	0.883	11.307	13.176	0.858	2.180	5475
	Tengchong	0.216	0.497	0.010	-	0.810	13.106	15.538	0.826	2.662	5471
	Average	0.236	0.517	0.030	-	0.886	9.878	12.121	0.892	1.886	5410
Bahell	Jiuquan	0.220	0.593	−0.281	0.218	0.948	8.616	10.003	0.900	1.549	5469
	Minqin	0.194	0.642	−0.348	0.263	0.951	7.616	9.325	0.928	1.192	5466
	Gangcha	0.188	0.766	−0.409	0.269	0.916	8.490	10.971	0.941	1.143	5430
	Xining	0.192	0.923	−0.968	0.629	0.940	9.645	10.965	0.911	1.346	5458
	Shiquanhe	0.236	0.827	−0.670	0.473	0.858	8.191	11.365	0.887	2.679	5433
	Naqu	0.281	0.554	−0.052	0.074	0.818	9.674	13.082	0.893	2.195	5294
	Lhasa	0.263	0.651	−0.206	0.105	0.885	6.837	8.945	0.885	2.318	5283
	Yushu	0.253	0.454	0.061	0.053	0.914	9.000	10.744	0.926	1.306	5473
	Guoluo	0.251	0.649	−0.373	0.316	0.889	9.429	12.001	0.911	1.635	5456
	Changdu	0.233	0.683	−0.603	0.614	0.876	9.122	11.606	0.882	2.016	5468
	Ganzi	0.272	0.698	−0.395	0.233	0.886	8.667	10.993	0.877	2.241	5068
	Ermeishan	0.230	0.775	−0.650	0.469	0.828	18.236	21.186	0.887	1.677	5472
	Lijiang	0.202	0.827	−0.726	0.477	0.894	9.984	11.144	0.871	2.126	5440
	Panzhihua	0.150	0.954	−1.193	0.805	0.888	11.065	12.912	0.870	1.991	5475
	Tengchong	0.203	0.787	−0.834	0.604	0.816	13.124	15.294	0.824	2.669	5471
	Average	0.225	0.719	−0.510	0.373	0.887	9.846	12.036	0.893	1.872	5410
Temperature-Based Models	**Station**	***a***	***b***	***c***	***d***	***NSE***	***MAPE***	***RRMSE***	***Slope***	***Inter***	***n***
Bristow	Jiuquan	0.758	0.036	1.423	-	0.755	14.467	21.719	0.804	3.527	5469
	Minqin	0.713	0.025	1.650	-	0.705	14.155	22.778	0.777	4.159	5466
	Gangcha	0.741	0.005	2.340	-	0.661	15.109	21.989	0.719	4.965	5429
	Xining	0.690	0.022	1.607	-	0.749	14.345	22.441	0.738	4.166	5458
	Shiquanhe	0.856	0.027	1.610	-	0.723	11.593	15.877	0.774	5.351	5433
	Naqu	0.903	0.045	1.245	-	0.519	16.620	21.285	0.620	7.452	5294
	Lhasa	0.769	0.012	1.974	-	0.661	11.639	15.377	0.740	5.581	5283
	Yushu	0.722	0.028	1.496	-	0.701	16.111	20.049	0.662	5.741	5473
	Guoluo	0.735	0.025	1.560	-	0.655	16.937	21.211	0.676	5.801	5456
	Changdu	1.005	0.030	1.181	-	0.686	14.739	18.464	0.688	5.164	5468
	Ganzi	0.785	0.026	1.512	-	0.723	13.688	17.092	0.752	4.709	5068
	Ermeishan	0.816	0.041	1.531	-	0.583	23.508	33.029	0.671	4.568	5472
	Lijiang	0.760	0.014	1.878	-	0.679	16.130	19.395	0.733	4.449	5440
	Panzhihua	0.601	0.010	2.123	-	0.664	16.205	22.377	0.642	5.693	5475
	Tengchong	0.917	0.057	1.118	-	0.619	18.363	21.991	0.699	4.725	5471
	Average	0.785	0.027	1.617	-	0.672	15.574	21.005	0.713	5.070	5410
Hargreaves	Jiuquan	0.184	−0.102	-	-	0.776	14.499	20.742	0.824	3.179	5469
	Minqin	0.172	−0.050	-	-	0.722	14.737	22.113	0.782	4.040	5466
	Gangcha	0.242	−0.251	-	-	0.692	14.909	20.958	0.739	4.832	5429
	Xining	0.175	−0.136	-	-	0.759	14.747	21.996	0.734	4.126	5458
	Shiquanhe	0.163	0.106	-	-	0.711	12.082	16.192	0.758	5.680	5433
	Naqu	0.175	−0.032	-	-	0.504	17.410	21.627	0.624	7.465	5294
	Lhasa	0.188	−0.047	-	-	0.651	12.350	15.621	0.708	6.054	5283
	Yushu	0.155	−0.038	-	-	0.686	16.832	20.554	0.653	5.917	5473
	Guoluo	0.151	−0.010	-	-	0.619	18.226	22.268	0.631	6.559	5456
	Changdu	0.182	−0.175	-	-	0.673	15.143	18.824	0.696	5.248	5468
	Ganzi	0.185	−0.115	-	-	0.712	14.173	17.425	0.740	4.864	5068
	Ermeishan	0.282	−0.306	-	-	0.622	23.526	31.451	0.680	4.437	5472
	Lijiang	0.258	−0.321	-	-	0.662	16.777	19.916	0.695	5.339	5440
	Panzhihua	0.214	−0.257	-	-	0.649	16.585	22.858	0.598	6.247	5475
	Tengchong	0.212	−0.192	-	-	0.625	18.203	21.811	0.703	4.662	5471
	Average	0.193	−0.128	-	-	0.671	16.013	20.957	0.704	5.243	5410

Table 1. *Cont.*

Temperature-Based Models	Station	*a*	*b*	*c*	*d*	*NSE*	*MAPE*	*RRMSE*	*Slope*	*Inter*	*n*
Chen	Jiuquan	0.312	−0.231	-	-	0.777	14.492	20.717	0.821	3.218	5469
	Minqin	0.300	−0.191	-	-	0.728	14.397	21.889	0.788	3.924	5466
	Gangcha	0.406	−0.409	-	-	0.700	14.690	20.672	0.763	4.469	5429
	Xining	0.302	−0.263	-	-	0.764	14.320	21.773	0.751	3.975	5458
	Shiquanhe	0.301	−0.072	-	-	0.714	12.058	16.127	0.770	5.463	5433
	Naqu	0.319	−0.211	-	-	0.508	17.359	21.538	0.638	7.199	5294
	Lhasa	0.345	−0.248	-	-	0.659	12.157	15.440	0.725	5.735	5283
	Yushu	0.282	−0.195	-	-	0.689	16.663	20.432	0.663	5.747	5473
	Guoluo	0.281	−0.174	-	-	0.635	17.623	21.813	0.661	6.022	5456
	Changdu	0.337	−0.374	-	-	0.673	15.279	18.837	0.708	5.039	5468
	Ganzi	0.335	−0.296	-	-	0.720	13.879	17.206	0.758	4.581	5068
	Ermeishan	0.357	−0.233	-	-	0.596	24.940	32.491	0.683	4.501	5472
	Lijiang	0.393	−0.397	-	-	0.662	16.699	19.920	0.717	4.924	5440
	Panzhihua	0.332	−0.330	-	-	0.657	16.159	22.616	0.620	5.957	5475
	Tengchong	0.293	−0.179	-	-	0.607	19.147	22.317	0.714	4.504	5471
	Average	0.326	−0.254	-	-	0.673	15.991	20.919	0.719	5.017	5410

The calibrated coefficients of the site-dependent models were then used to predict daily solar irradiation at different stations, and the model performance is shown in Table 2. Comparison between Tables 1 and 2 indicates that model prediction performed a little worse for the validation period compared to the calibration period for both sunshine- and temperature-based models, which is a normal phenomenon in the view of statistical theory [45]. However, changes in *NSE* and the other evaluation indicators within and between the sunshine- and temperature-based models are quite similar to those for the calibration period. Differences in model performance were further analyzed by *t*-test (Figure 2), and the results indicate lower *t* values exist within the results from sunshine- or temperature-based models, but the *t* value is greater between the results from sunshine- and temperature-based models (though not significant with $t_{0.05}$ test), showing great difference exists between the performance of the sunshine- and temperature-based models.

Table 2. Validation of the sunshine- and temperature-based site-dependent models for the calibrated coefficients in Table 1 using data from 2008 to 2010 at different locations in this study.

Sunshine-Based Models	Station	*NSE*	*MAPE*	*RRMSE*	*Slope*	*Inter*	*n*
Angtrom	Jiuquan	0.949	9.886	10.474	0.918	1.640	1095
	Minqin	0.958	8.603	9.101	0.925	1.490	1096
	Gangcha	0.935	7.937	9.211	0.996	−0.123	1096
	Xining	0.926	9.919	11.615	0.908	1.414	1095
	Shiquanhe	0.900	6.956	8.896	0.972	0.336	1090
	Naqu	0.872	8.723	10.344	0.940	1.387	1094
	Lhasa	0.891	6.772	8.510	0.919	2.174	1094
	Yushu	0.815	15.476	16.710	0.879	2.871	731
	Guoluo	0.813	10.895	15.672	0.889	2.401	1095
	Changdu	0.801	14.128	15.551	0.872	3.115	1094
	Ganzi	0.914	8.226	9.582	0.878	2.208	1096
	Ermeishan	0.876	16.952	17.767	0.890	1.679	1096
	Lijiang	0.838	11.840	13.555	0.890	2.074	1096
	Panzhihua	0.700	20.535	22.453	0.702	4.236	1096
	Tengchong	0.781	14.395	15.943	0.885	3.037	1096
	Average	0.865	11.416	13.026	0.898	1.996	1070

Table 2. *Cont*.

Sunshine-Based Models	Station	*NSE*	*MAPE*	*RRMSE*	*Slope*	*Inter*	*n*
Ogelman	Jiuquan	0.949	9.825	10.414	0.919	1.651	1095
	Minqin	0.958	8.355	9.084	0.925	1.499	1096
	Gangcha	0.935	7.935	9.212	0.995	−0.117	1096
	Xining	0.927	10.143	11.512	0.908	1.359	1095
	Shiquanhe	0.902	6.863	8.827	0.967	0.477	1090
	Naqu	0.872	8.741	10.346	0.936	1.471	1094
	Lhasa	0.890	6.795	8.537	0.921	2.142	1094
	Yushu	0.818	15.418	16.593	0.882	2.833	731
	Guoluo	0.814	10.952	15.628	0.880	2.531	1095
	Changdu	0.801	14.063	15.550	0.864	3.245	1094
	Ganzi	0.914	8.134	9.532	0.884	2.100	1096
	Ermeishan	0.875	16.975	17.799	0.891	1.685	1096
	Lijiang	0.836	12.131	13.627	0.896	1.982	1096
	Panzhihua	0.699	20.475	22.483	0.702	4.233	1096
	Tengchong	0.781	14.382	15.918	0.885	3.035	1096
	Average	0.865	11.412	13.004	0.897	2.008	1070
Bahell	Jiuquan	0.949	9.924	10.415	0.921	1.612	1095
	Minqin	0.959	8.564	9.038	0.925	1.492	1096
	Gangcha	0.936	7.900	9.178	0.996	−0.118	1096
	Xining	0.930	9.778	11.289	0.916	1.269	1095
	Shiquanhe	0.903	6.861	8.778	0.963	0.577	1090
	Naqu	0.872	8.736	10.338	0.934	1.501	1094
	Lhasa	0.891	6.859	8.501	0.919	2.165	1094
	Yushu	0.816	15.483	16.683	0.885	2.827	731
	Guoluo	0.813	10.940	15.637	0.877	2.592	1095
	Changdu	0.801	14.199	15.551	0.868	3.215	1094
	Ganzi	0.915	8.095	9.501	0.884	2.110	1096
	Ermeishan	0.878	16.722	17.617	0.885	1.754	1096
	Lijiang	0.842	12.016	13.379	0.897	1.951	1096
	Panzhihua	0.701	20.488	22.407	0.712	4.074	1096
	Tengchong	0.788	14.425	15.675	0.874	3.173	1096
	Average	0.866	11.399	12.932	0.897	2.013	1070
Temperature-Based Models	**Station**	***NSE***	***MAPE***	***RRMSE***	***Slope***	***Inter***	***n***
Bristow	Jiuquan	0.770	14.855	22.153	0.817	3.348	1095
	Minqin	0.717	14.707	23.708	0.778	4.224	1096
	Gangcha	0.695	15.157	19.997	0.776	4.072	1096
	Xining	0.753	13.420	21.190	0.756	4.077	1095
	Shiquanhe	0.766	10.497	13.621	0.825	4.154	1090
	Naqu	0.575	15.823	18.860	0.667	6.465	1094
	Lhasa	0.694	10.964	14.229	0.753	5.398	1094
	Yushu	0.657	20.469	22.767	0.644	6.141	731
	Guoluo	0.566	18.112	23.834	0.660	6.283	1095
	Changdu	0.684	17.803	19.600	0.695	5.533	1094
	Ganzi	0.746	13.516	16.429	0.755	4.505	1096
	Ermeishan	0.648	22.507	29.902	0.675	4.416	1096
	Lijiang	0.575	18.449	21.923	0.736	5.345	1096
	Panzhihua	0.476	22.951	29.656	0.489	8.016	1096
	Tengchong	0.591	18.538	21.779	0.744	4.344	1096
	Average	0.661	16.518	21.310	0.718	5.088	1070

Table 2. *Cont.*

Temperature-Based Models	Station	*NSE*	*MAPE*	*RRMSE*	*Slope*	*Inter*	*n*
Hargreaves	Jiuquan	0.797	14.732	20.811	0.837	3.050	1095
	Minqin	0.730	14.999	23.129	0.774	4.230	1096
	Gangcha	0.725	15.089	18.977	0.792	4.018	1096
	Xining	0.759	13.944	20.907	0.752	4.054	1095
	Shiquanhe	0.735	11.177	14.485	0.804	4.646	1090
	Naqu	0.544	16.754	19.546	0.663	6.619	1094
	Lhasa	0.684	11.631	14.472	0.714	5.999	1094
	Yushu	0.628	21.701	23.705	0.620	6.619	731
	Guoluo	0.532	19.659	24.756	0.613	7.099	1095
	Changdu	0.666	18.483	20.152	0.712	5.496	1094
	Ganzi	0.752	13.904	16.225	0.747	4.609	1096
	Ermeishan	0.677	22.551	28.612	0.688	4.197	1096
	Lijiang	0.492	20.909	23.983	0.706	6.213	1096
	Panzhihua	0.486	22.959	29.388	0.473	8.143	1096
	Tengchong	0.601	18.056	21.514	0.753	4.222	1096
	Average	0.654	17.103	21.377	0.710	5.281	1070
Chen	Jiuquan	0.797	14.521	20.787	0.836	3.004	1095
	Minqin	0.734	14.715	22.976	0.784	4.069	1096
	Gangcha	0.732	14.787	18.721	0.816	3.667	1096
	Xining	0.762	13.723	20.789	0.767	3.884	1095
	Shiquanhe	0.738	11.070	14.417	0.818	4.342	1090
	Naqu	0.545	16.725	19.531	0.683	6.254	1094
	Lhasa	0.691	11.553	14.307	0.733	5.645	1094
	Yushu	0.632	21.368	23.572	0.636	6.374	731
	Guoluo	0.544	18.873	24.430	0.643	6.596	1095
	Changdu	0.663	18.460	20.236	0.733	5.171	1094
	Ganzi	0.763	13.301	15.854	0.772	4.204	1096
	Ermeishan	0.655	23.907	29.607	0.688	4.261	1096
	Lijiang	0.502	20.275	23.736	0.714	5.946	1096
	Panzhihua	0.488	22.858	29.311	0.481	8.050	1096
	Tengchong	0.569	19.433	22.354	0.764	4.033	1096
	Average	0.654	17.038	21.375	0.725	5.033	1070

On the whole, the sunshine-based models performed better than the temperature-based ones, but only small differences in model performance exit within sunshine- or temperature-based models themselves. So the highly rated Ångström and Bristow models, representing the sunshine- and temperature-based model respectively, were selected for further study on developing average and geographical models in the following sections.

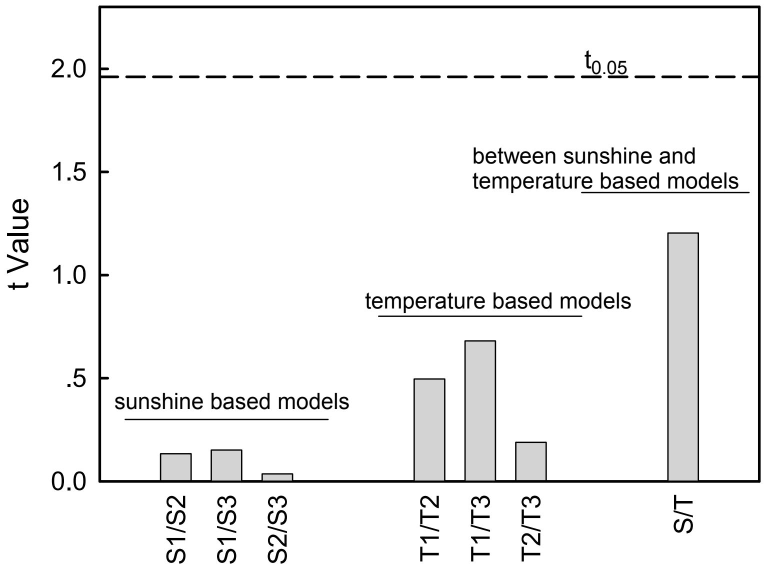

Figure 2. Values of *t*-statistic test between and within the results from the sunshine- and temperature-based model. S1, S2, S3 denote the sunshine-based model Angstrom, Ogelman and Bahell, respectively. T1, T2, T3 denote the temperature-based model Bristow, Hargreaves and Chen, respectively.

2.2.2. Average Models

Regional coefficients of *a* and *b* in the Ångström model were obtained by simply averaging the coefficients calibrated at the fifteen radiation stations, then daily solar irradiation was predicted at each station by the same coefficients of *a* and *b*, with values of 0.229 and 0.549 respectively. As mentioned above, the coefficients of *a* and *b* vary greatly between different stations, thus using the average coefficients to represent all of the coefficients at the fifteen stations will cause bigger error than the models with site-dependent coefficients. Comparison of Tables 2 and 3 shows the difference in model performance at all the stations for the Ångström model. The average *NSE* of the simple average mode is 0.826, also lower than the corresponding value of 0.865 in the site-dependent model. The two smallest values of *NSE* validated by the site-dependent model is 0.700 in Panzhihua and 0.781 in Tengchong, while the two smallest values of *NSE* validated by the simple average model are only 0.586 in Tengchong and 0.596 in Panzhihua, respectively. Performance of the Bristow-type simple average model is also shown in Table 3. No values of the *NSE* were lower than 0.400 in the performance of the site-dependent Bristow model (Table 2), whereas there are 5 out of 15 stations with *NSE* values lower than 0.400 for the Bristow-type simple average model (Table 3).

Performance of the statistical average model can also be seen in Table 3. The coefficients of *a* and *b* in the Ångström-type statistical model are 0.229 and 0.550 respectively, nearly the same as those in the corresponding simple average model. Estimation of daily solar irradiation at 15 stations with the nearly same coefficients leads to a very similar model performance between Ångström-type simple average model and the corresponding statistical average model (Table 3). In contrast, the coefficients of the Bristow-type statistical average model are quite different from those of the Bristow-type simple average model. All in all, the Bristow-type statistical average model performed better than the Bristow-type simple average model at 11 out of 15 stations based on *NSE* (Table 3).

Table 3. Performance of the simple average model and the statistical average model using the validation dataset from 2008 to 2010. (A) Simple average model. Angstrom-Based model: a = 0.229, b = 0.549; Browstow-Based model: a = 0.785, b = 0.027, c = 1.617. (B) Statistical average model. Angstrom-based model: a = 0.229, b = 0.550; Browstow-Based model: a = 0.757, b = 0.044, c = 1.373.

(A)

Station	Angstrom-Based Model						Bristow-Based Model					
	NSE	*MAPE*	*RRMSE*	*Slope*	*Inter*	*n*	*NSE*	*MAPE*	*RRMSE*	*Slope*	*Inter*	*n*
Jiuquan	0.922	12.707	12.874	0.976	1.692	1095	0.656	17.055	27.051	0.902	3.917	1095
Minqin	0.923	11.950	12.368	0.971	1.938	1096	0.618	16.603	27.514	0.852	4.681	1096
Gangcha	0.935	8.319	9.221	0.950	0.581	1096	0.667	15.822	20.872	0.736	5.283	1096
Xining	0.914	10.315	12.476	0.946	1.570	1095	0.381	23.436	33.553	0.881	5.700	1095
Shiquanhe	0.813	10.635	12.165	0.891	0.524	1090	0.704	13.217	15.323	0.760	3.841	1090
Naqu	0.803	11.043	12.850	0.876	0.811	1094	0.512	17.045	20.216	0.702	6.729	1094
Lhasa	0.873	7.226	9.158	0.887	1.515	1094	0.697	11.031	14.165	0.726	5.765	1094
Yushu	0.825	15.188	16.279	0.865	2.896	731	0.241	29.879	33.854	0.755	7.800	731
Guoluo	0.823	10.975	15.224	0.859	2.113	1095	0.254	23.070	31.258	0.734	7.618	1095
Changdu	0.829	13.335	14.398	0.833	3.365	1094	−0.340	35.835	40.364	0.844	7.929	1094
Ganzi	0.852	10.014	12.526	0.875	0.940	1096	0.574	17.311	21.276	0.812	5.682	1096
Ermeishan	0.875	16.921	17.825	0.865	1.679	1096	0.532	27.520	34.454	0.628	2.670	1096
Lijiang	0.821	12.766	14.228	0.909	2.192	1096	0.463	20.612	24.653	0.691	7.032	1096
Panzhihua	0.596	21.462	26.031	0.787	5.722	1096	0.278	22.468	34.809	0.555	10.352	1096
Tengchong	0.586	20.136	21.910	0.960	3.153	1096	0.421	21.466	25.898	0.913	2.689	1096
Average	0.826	12.866	14.636	0.897	2.046	1070	0.444	20.825	27.017	0.766	5.846	1070

(B)

Station	Angstrom-Based Model						Bristow-Based Model					
	NSE	*MAPE*	*RRMSE*	*Slope*	*Inter*	*n*	*NSE*	*MAPE*	*RRMSE*	*Slope*	*Inter*	*n*
Jiuquan	0.921	12.791	12.954	0.977	1.690	1095	0.755	14.536	22.848	0.821	3.726	1095
Minqin	0.922	12.051	12.456	0.972	1.936	1096	0.712	14.461	23.882	0.775	4.441	1096
Gangcha	0.935	8.289	9.201	0.951	0.576	1096	0.653	17.301	21.314	0.661	5.147	1096
Xining	0.914	10.365	12.519	0.947	1.566	1095	0.605	16.586	26.807	0.799	5.517	1095
Shiquanhe	0.816	10.557	12.086	0.892	0.522	1090	0.483	17.777	20.253	0.690	3.713	1090
Naqu	0.805	10.986	12.787	0.877	0.805	1094	0.554	16.502	19.333	0.631	6.466	1094
Lhasa	0.875	7.182	9.112	0.888	1.514	1094	0.602	12.814	16.229	0.655	5.526	1094
Yushu	0.824	15.212	16.314	0.867	2.894	731	0.510	24.994	27.207	0.682	7.381	731
Guoluo	0.823	10.962	15.218	0.860	2.108	1095	0.478	20.002	26.138	0.661	7.376	1095
Changdu	0.829	13.367	14.433	0.834	3.363	1094	0.204	27.992	31.115	0.767	7.475	1094
Ganzi	0.853	9.965	12.472	0.877	0.934	1096	0.716	14.602	17.374	0.731	5.540	1096
Ermeishan	0.875	16.904	17.809	0.866	1.670	1096	0.469	27.786	36.721	0.542	3.555	1096
Lijiang	0.820	12.814	14.271	0.911	2.183	1096	0.575	18.558	21.942	0.593	7.316	1096
Panzhihua	0.594	21.437	26.101	0.788	5.721	1096	0.428	21972	30.982	0.485	9.995	1096
Tengchong	0.582	20.240	22.011	0.961	3.144	1096	0.582	18.985	22.013	0.781	3.655	1096
Average	0.826	12.875	14.650	0.898	2.042	1070	0.555	18.991	24.277	0.685	5.789	1070

In short, the Ångström-type simple average model performs nearly the same as the Ångström-type statistical average model, and both of the models are better than the Bristow-type simple/statistical average models. Among all of the average models, the Bristow-type simple average model performed the worst, even having a negative *NSE* value at Changdu station.

2.2.3. Geographical Models

Coefficients of the site-dependent Ångström/Bristow models at 15 stations (Table 1) were fitted with their corresponding geographical parameters, and the multiple linear models linking the coefficients and the geographical parameters were shown in Table 4.

Table 4. Coefficient estimation for the Angstrom- and Bristow-type geographical models.

Model	Coefficient	Multiple Linear Model	R^2
Angstrom	*a*	$0.136561 + 0.000578 \times \text{Lon} - 0.000821 \times \text{Lat} + 2.155 \times 10^{-5} \times \text{Alt}$	0.473
	b	$0.504951 - 0.000858 \times \text{Lon} + 0.002200 \times \text{Lat} + 1.968 \times 10^{-5} \times \text{Alt}$	0.548
Bristow	*a*	$1.216623 - 0.003490 \times \text{Lon} - 0.005194 \times \text{Lat} + 2.641 \times 10^{-5} \times \text{Alt}$	0.264
	b	$0.058410 - 0.000149 \times \text{Lon} - 0.000519 \times \text{Lat} - 8.278 \times 10^{-8} \times \text{Alt}$	0.033
	c	$1.237263 + 0.002983 \times \text{Lon} + 0.005364 \times \text{Lat} - 2.933 \times 10^{-5} \times \text{Alt}$	0.024

Lon: Longitude, (°E); Lat: Latitude, (°N); Alt: Altitude, (m).

The geographical models are somewhat more complex than the simple/statistical average models with more geographical parameters involved. Thus, the geographic model would be expected to perform better than the simple/statistical average models. However, Ångström-type geographical model performs almost the same as the corresponding average models, while the Bristow-type geographical model performed better than the corresponding simple average model but worse than the statistic one (Table 5). In addition, the better performed Ångström-type geographical model cannot be applicable under extreme conditions, e.g., in the mountain Everest with altitude 8844.43 m, due to its unacceptable coefficient (a + b) greater than 1. This will be further discussed in the below sections.

Table 5. Performance of the Angstrom- and Bristow-type geographical models using validation dataset from 2008 to 2010.

Model	Station	*a*	*b*	*c*	*NSE*	*MAPE*	*RRMSE*	*Slope*	*Inter*	*n*
Angstrom	Jiuquan	0.193	0.538	-	0.930	11.863	12.228	0.992	1.174	1095
	Minqin	0.195	0.529	-	0.958	8.316	9.153	0.910	1.538	1096
	Gangcha	0.236	0.567	-	0.934	7.971	9.305	0.981	0.593	1096
	Xining	0.216	0.544	-	0.923	10.270	11.857	0.941	1.331	1095
	Shiquanhe	0.250	0.593	-	0.871	8.624	10.107	0.917	0.703	1090
	Naqu	0.270	0.591	-	0.863	8.952	10.708	0.961	1.274	1094
	Lhasa	0.245	0.565	-	0.895	6.617	8.328	0.929	1.657	1094
	Yushu	0.247	0.568	-	0.752	17.591	19.335	0.909	3.230	731
	Guoluo	0.248	0.569	-	0.807	11.027	15.911	0.897 0.996 0.851	2.395	1095
	Changdu	0.240	0.556	-	0.802	14.410	15.508	0.851	3.551	1094
	Ganzi	0.243	0.557	-	0.777	12.591	15.381	0.864	0.451	1096
	Ermeishan	0.239	0.542	-	0.802	20.055	22.424	0.867	3.521	1096
	Lijiang	0.225	0.526	-	0.841	11.725	13.409	0.872	2.269	1096
	Panzhihua	0.200	0.500	-	0.468	24.083	29.885	0.745	7.451	1096
	Tengchong	0.209	0.509	-	0.757	14.848	16.786	0.925	2.647	1096
	Average	0.230	0.550	-	0.825	12.596	14.688	0.904	2.252	1070
Bristow	Jiuquan	0.705	0.023	1.701	0.757	14.819	22.757	0.823	3.583	1095
	Minqin	0.692	0.023	1.712	0.718	14.901	23.655	0.767	4.275	1096
	Gangcha	0.759	0.024	1.640	0.684	15.991	20.345	0.702	4.860	1096
	Xining	0.730	0.024	1.671	0.578	17.405	27.684	0.828	5.258	1095
	Shiquanhe	0.880	0.029	1.526	0.771	10.666	13.482	0.809	4.037	1090
	Naqu	0.857	0.028	1.541	0.463	17.444	21.201	0.734	6.715	1094
	Lhasa	0.839	0.029	1.562	0.657	12.031	15.058	0.755	6.065	1094
	Yushu	0.802	0.027	1.597	0.228	30.071	34.148	0.763	7.742	731
	Guoluo	0.784	0.025	1.613	0.356	21.858	29.041	0.727	7.192	1095
	Changdu	0.802	0.027	1.598	−0.395	36.530	41.179	0.857	7.890	1094
	Ganzi	0.792	0.027	1.607	0.574	17.403	21.271	0.816	5.628	1096
	Ermeishan	0.782	0.027	1.615	0.524	27.790	34.743	0.624	2.651	1096
	Lijiang	0.790	0.029	1.611	0.362	22.650	26.870	0.693	7.561	1096
	Panzhihua	0.755	0.029	1.649	0.231	23.586	35.933	0.545	10.828	1096
	Tengchong	0.786	0.031	1.617	0.252	23.273	29.434	0.924	3.580	1096
	Average	0.784	0.027	1.617	0.451	20.428	26.453	0.758	5.858	1070

2.2.4. Improved Ångström-Type Model

As mentioned above, the sunshine-based Ångström model is superior to the temperature-based Bristow model. Therefore, the Ångström model was selected to develop a new model for regional application on the TP and its surrounding regions. For development of the regional model, suitable equations should be established to account for the variations in the coefficients of Ångström model on the TP and its surrounding regions. Therefore, variations in the coefficients of Ångström model was analyzed first. Coefficients of a, b and $(a + b)$ at 15 radiation stations are given in Figure 3, indicating not only a and b but also the sum of $(a + b)$ vary greatly on the TP and its surrounding regions.

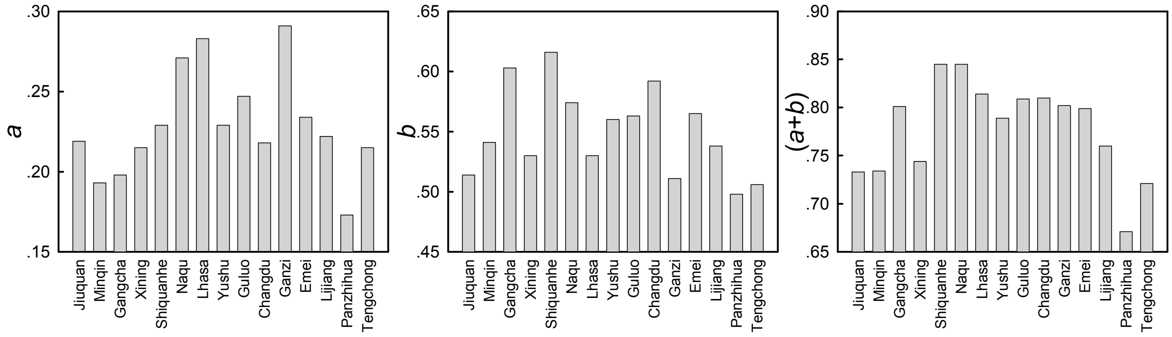

Figure 3. Variation in coefficients of the site-dependent Ångström model.

To account for the great variation in the coefficients in Figure 3, more than one hundred of different mathematical functions and variable combinations were tested to find the best equation to fit the relationship between coefficients of Ångström model and the related geographical or meteorological factors. The leading factor accounting for the variation in coefficient b was identified as water vapor pressure, and a reciprocal relation was established between the coefficient b and the corresponding averaged daily water vapor pressure (Figure 4a). We failed to find the suitable equation for fitting the coefficient a, though it is believed that coefficient a is related to cloudiness [42]. However, it was found that the sum of coefficients $(a + b)$ correlated well to the altitude as a logarithm function (Figure 4b). Thus, the improved Ångström-type model can be expressed as follows:

$$\frac{H}{H_0} = a + b\frac{S}{S_0} \quad (1)$$

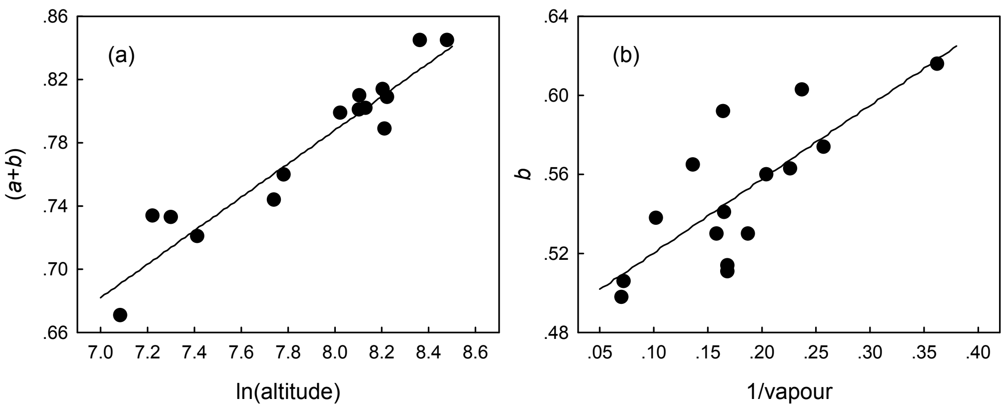

Figure 4. Relationship between coefficients in the Ångström model and the leading factors related to (**a**) altitude (m), and (**b**) water vapor pressure (hPa).

If $S = S_0$, i.e., cloud-free conditions, then $H = (a + b)H_0$. Since the clearness index Kt is defined as $H = KtH_0$, $(a + b) = Kt$ in the cloud-free conditions. When $S = 0$, i.e., overcast conditions, then $H = aH_0$, and a is equal to Kt in overcast conditions.

$$a + b = 0.106 \times \ln(Alt) - 0.060 \tag{2}$$

$$b = 0.373 \times \frac{1}{Vap} + 0.483 \tag{3}$$

where Alt is altitude (m), and Vap is the average daily water vapor pressure (hPa). Linear regressions between coefficients and leading factors indicate that the improved model accounts fairly well for variations in the coefficients of the Ångström model (Figure 4).

Validation of the improved Ångström-type model indicates that it performs better than the average and geographical models (Table 6). In addition, the improved Ångström-type model can also account for the variations in coefficients better than the average and geographical models. Performance of the different kinds of models in predicting annual mean of daily solar irradiation at Lhasa in the validation period 2008–2010 is shown in Figure 5, indicating vividly that improved Ångström-type model performs much better than the average and geographical models. Note that it is only fortuitous that the *NSE* of the geographical model is even greater than those of the site-dependent Ångström, Ogelman and Bahell models. The *NSE* values of the improved Ångström-type model are generally slightly lower than those of the site-dependent models (Tables 2 and 6). Figures drawn for the other stations are quite similar to Figure 5, and were not shown due to the limitation of space.

Table 6. Performance of the improved Ångström-type model.

Station	*a*	*b*	*NSE*	*MAPE*	*RRMSE*	*Slope*	*Inter*	*n*
Jiuquan	0.167	0.546	0.941	9.687	11.169	0.908	0.941	1095
Minqin	0.160	0.545	0.947	8.807	10.236	0.898	1.059	1096
Gangcha	0.226	0.571	0.937	7.931	9.091	0.977	0.431	1096
Xining	0.217	0.542	0.925	10.010	11.660	0.926	1.398	1095
Shiquanhe	0.207	0.618	0.883	7.963	9.642	0.953	0.131	1090
Naqu	0.259	0.579	0.877	8.571	10.157	0.937	1.154	1094
Lhasa	0.256	0.553	0.898	6.538	8.225	0.919	1.817	1094
Yushu	0.250	0.559	0.771	17.150	18.600	0.895	3.255	731
Guoluo	0.243	0.567	0.814	10.836	15.608	0.891	2.307	1095
Changdu	0.254	0.544	0.784	15.196	16.212	0.849	3.814	1094
Ganzi	0.255	0.546	0.900	8.376	10.286	0.893	1.401	1096
Ermeishan	0.256	0.534	0.861	18.039	18.753	0.848	2.618	1096
Lijiang	0.243	0.521	0.826	12.681	14.041	0.867	2.860	1096
Panzhihua	0.181	0.509	0.710	19.882	22.084	0.719	4.444	1096
Tengchong	0.215	0.510	0.773	14.598	16.214	0.892	3.005	1096
Average	0.226	0.550	0.856	11.751	13.465	0.891	2.042	1070

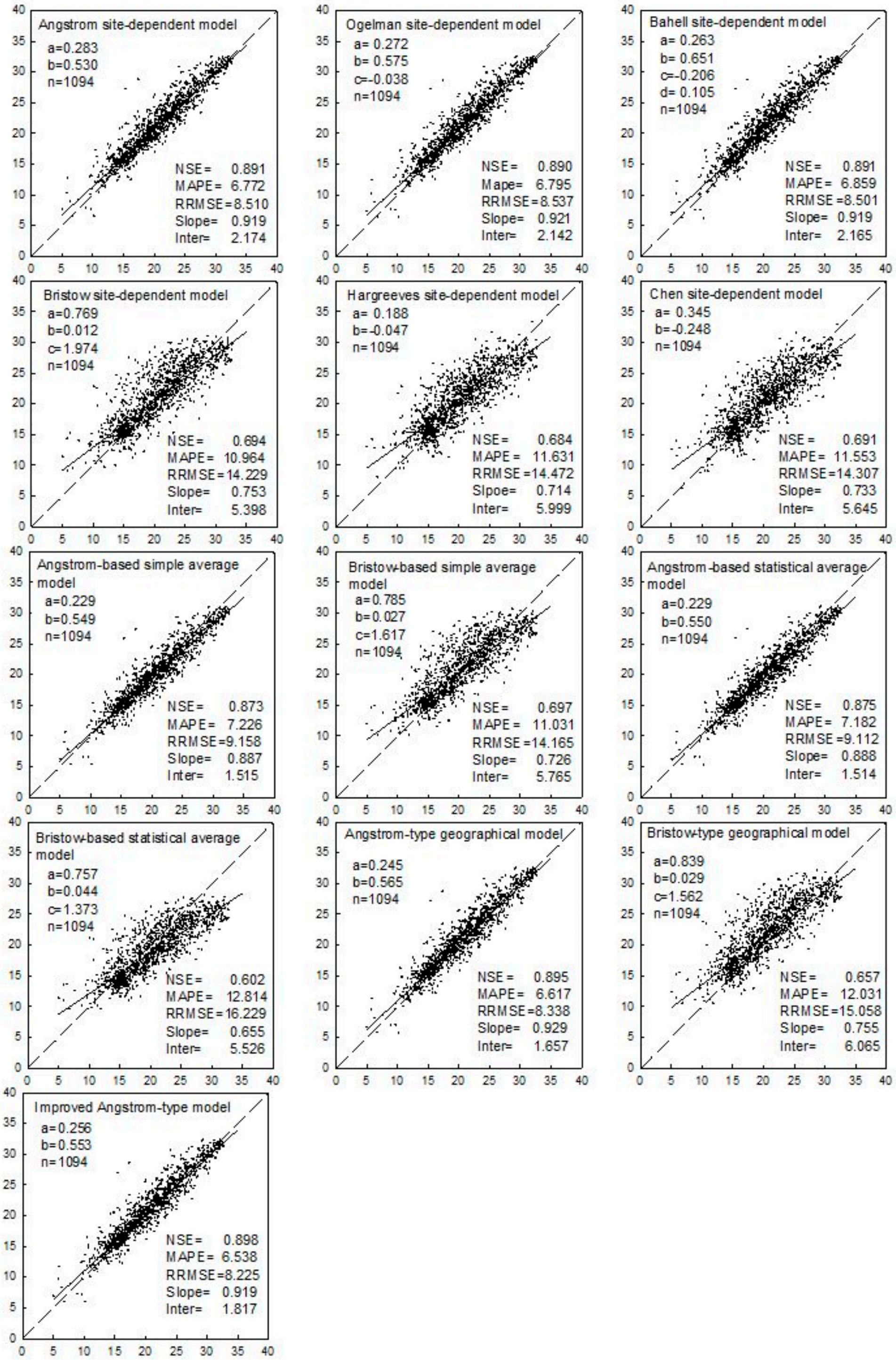

Figure 5. Performance of different models in predicting daily solar irradiation in Lhasa from 2008 to 2010. The horizontal axis denotes observation values, and the vertical axis prediction values (unit: MJ·m^{-2}).

As mentioned above, the improved Ångström-type model performs much better than the average and geographical models, with higher skill in accounting for the coefficient variations. Thus, the improved Ångström-type model was selected to estimate the spatial distribution of the annual mean of daily solar irradiation on the TP.

2.3. Estimation of the Spatial Distribution of the Annual Mean of Daily Solar Irradiation with the Improved Ångström-Type Model

The spatial distribution of the annual mean of daily solar irradiation was estimated by the improved Ångström-type model using gridded 1 km × 1 km sunshine percentage and water vapor pressure interpolated over the region. The first step was to validate the ANUSPLIN interpolation method on the TP. To do so, water vapor pressure data measured at 8 stations in the period 1993–2010 were selected as a validation dataset. Then, water vapor pressure from the other weather stations was used as input to the ANUSPLIN software to interpolate the gridded water vapor pressure data over the TP. The interpolated water vapor pressure at the 8 selected stations in the period 1993–2010 were used to validate against the measured ones, and the result of the validation indicated that a reliable and accurate interpolation could be done by ANUSPLIN interpolation method (Figure 6a). Validation of the sunshine percentage showed similar result as that for water vapor pressure (Figure 6b).

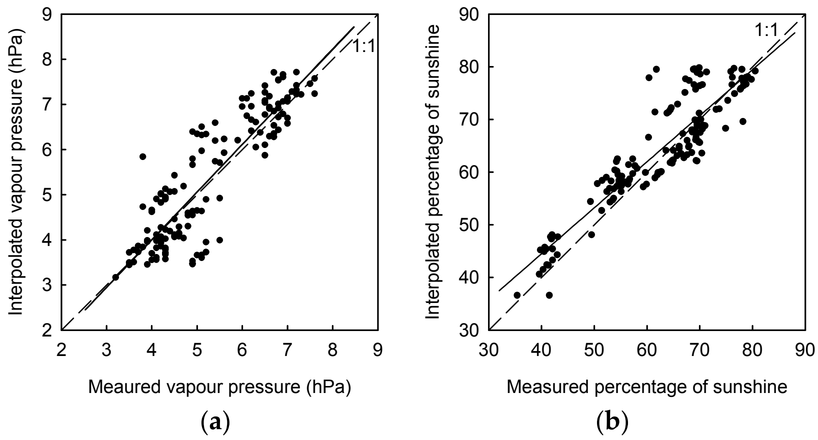

Figure 6. Validation of the ANUSPLIN method in interpolating (**a**) water vapor pressure and (**b**) sunshine percentage over the Tibetan Plateau and its surrounding regions.

Based on these results, the spatial distribution of water vapor pressure and sunshine percentage on the TP was interpolated (Figure 7b,c), based on which the coefficients of (a + b), b and a were rasterized by the improved Ångström-type model using the ArcGIS 10.3 platform (Figure 7e,f).

Extra-terrestrial radiation is defined as the solar radiation received at the top of the earth's atmosphere on a horizontal surface, and is only a function of latitude, date and length of the daytime. By accumulation of the time, the annual daily extra-terrestrial radiation should be distributed latitudinally. The extra-terrestrial radiation calculated according to Allen et al. [9] exactly fits this basic common knowledge (Figure 8a). Finally, the coefficients of a and b, sunshine percentage and the extra-terrestrial radiation were used as input variables to drive the improved Ångström-type model for estimation of the annual mean of daily solar irradiation on the TP. Both annual and seasonal spatial distribution of the annual mean of daily solar irradiation were rasterized in Figure 8b–f. Generally speaking, the annual mean of daily solar irradiation is greater in spring and summer and less in the autumn, and radiation increases from east to the west, with greatest values in the southwest part of the TP. The notable exception of the greatest annual mean of daily solar irradiation located in the most south TP for the winter in Figure 8f might be attributed to grater coefficients b aroused by the lower water vapor pressure and greater extra-terrestrial radiation in this region in winter days. Annual mean of daily solar irradiation has a similar spatial distribution to those of the seasonal, ranging from 9 MJ·m^{-2} in the east to the 24 MJ·m^{-2} in the southwest TP.

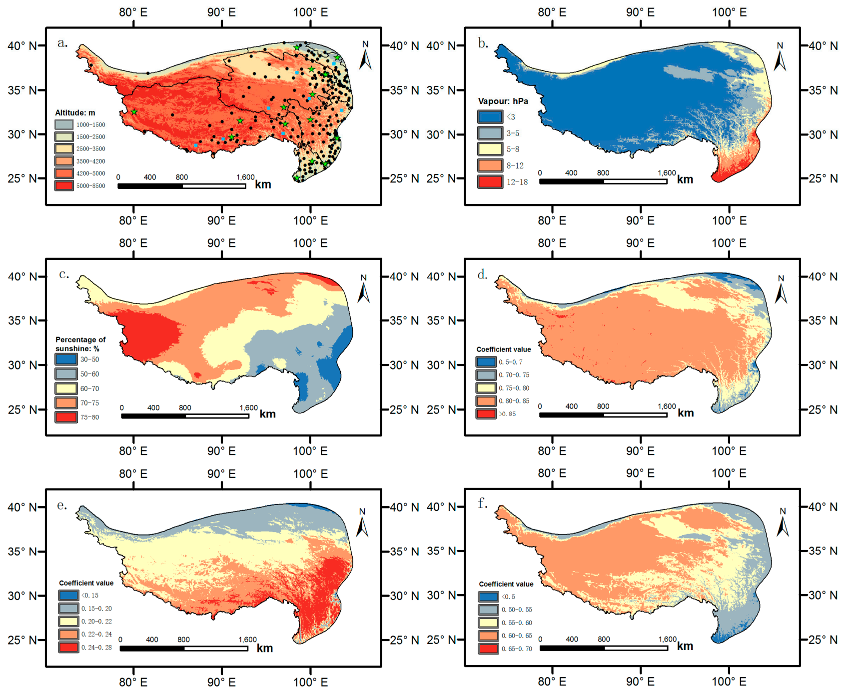

Figure 7. Distribution of weather stations, the interpolated meteorological variables and the rasterized coefficients of the Ångström model. (**a**) Distribution of weather stations, stars denote radiation stations, dots the weather stations, and squares weather station used for validation of ANUSPLIN method, (**b**) annual mean water vapor pressure (unit: hPa), (**c**) annual mean sunshine percentage, (**d**) coefficient (a + b), (**e**) coefficient a, and (**f**) coefficient b.

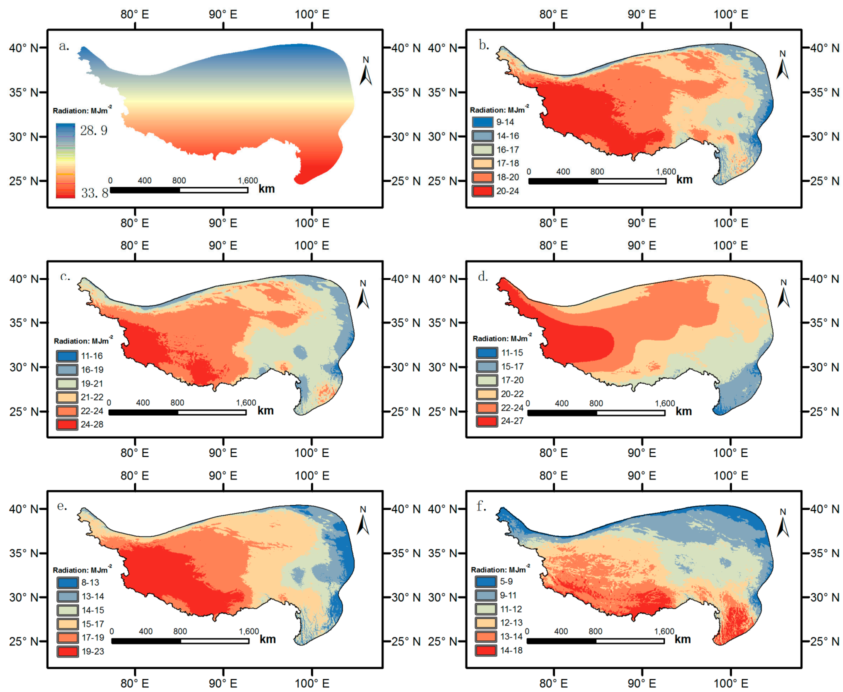

Figure 8. Spatial distribution of the annual mean of daily solar irradiation over the Tibetan Plateau. (**a**) Extra-terrestrial radiation, (**b**) Annual mean of daily solar irradiation, and the seasonal mean of daily solar irradiation in (**c**) spring, (**d**) summer, (**e**) autumn, and (**f**) winter (unit: MJ·m^{-2}).

3. Discussion

The main objective of this research is to develop a suitable method for estimating the annual mean of daily solar irradiation under complex terrain conditions like the TP. Based on the annual mean of daily solar irradiation measured over the TP and its surrounding regions, we have identified the variation of coefficients at different locations, and the performances among several methods on determining the regional coefficients were compared. These results are based on the strictly checked dataset and statistical analysis, and can be believed to be reliable with few uncertainties and limitations. The spatial distribution of the annual mean of daily solar irradiation was estimated based on the ANUSPLIN interpolation method and the improved Ångström-type model. The Ångström model performs better than the Bristow-Campbell model used in our previous study [52]. However, the inherent defects of the interpolation method and paucity of the observation data in the central and western TP would inevitably lead to some uncertainties in the estimation of the spatial distribution of the annual mean of solar irradiation on the TP. In what follows we will discuss these aspects in more detail.

3.1. Variation in the Coefficients of the Site-Dependent Models on the Tibetan Plateau

The coefficients of the site-dependent models used in this study are comparable to most of the results reported in previous studies [30,41,42], and the difference of the coefficients between different studies can be attributed to the differences in quality control and length of the dataset used for model calibration.

The coefficients of both sunshine- and temperature-based models vary more greatly than those reported on the plain regions e.g., [30,41,42,44,49,50], and the coefficients of the highly rated Ångström and Bristow models deserved to be discussed in more detail. The coefficients a and b of the Ångström model change considerably between stations at higher altitude compared to those at lower elevations (Figure 3), and the sum of the coefficients ($a + b$) increases from 0.671 in Panzhihua to 0.845 in Shiquanhe and Naqu. In contrast, the sum ($a + b$) of Ångström model only varies from 0.68 to 0.78 among 20 stations distributed in North and Northeast Plain of China [42]. The coefficients a and b of the Ångström model reflect the effect of type and thickness of prevailing clouds and the transmission characteristics of the atmosphere, which is mainly determined by the total water content and turbidity [42]. Due to the effect of monsoon and the complex terrain, the prevailing clouds differ greatly across the TP [55,56]. In addition, as the altitude of the ground increases, the thickness of the atmosphere above decreases, and the atmospheric transmittance increases as a whole (Equation (1)), which is the reason that ($a + b$) in the TP varies greater than the ($a + b$) in areas of lower terrain. As for the temperature-based Bristow model, the coefficients also change greatly on the TP and its surrounding regions (Table 1), in line with previous findings in [52]. In Bristow model, coefficient a represents the potential transmittance on a clear day, while coefficients b and c control the rate at which a is approached as the temperature difference increases [28,52]. For a clear sky condition, the transmittance is mainly determined by air mass, ozone, aerosol density and water vapor content [57]. Generally speaking, the TP can be treated as a clean region with lower aerosol density compared to other parts of China [58], so the effect of aerosol is relatively smaller. The ozone is distributed inhomogeneously with a lower center on the TP [59]. Though ozone has a large effect on the irradiation at short wavelength, it has a negligible influence on the total irradiation. However, the air mass could change greatly on the TP due to large elevation difference aroused by the complex terrain [54], which will surely contribute to a great variation in the coefficient a in Bristow model. Coefficients b and c of Bristow model control the changing rate in atmospheric transmissivity as diurnal temperature difference changes, which mean that both of them have close relation to the Diurnal Temperature Range (DTR) at a given station. DTR on the TP is much larger than that at the lower altitude, as solar radiation is greater in daytime and greenhouse effect of the atmosphere at night is very weak due to thin air in the higher elevation regions [55,60]. In addition, the rolling terrain on the TP also leads to the different DTR at different locations, e.g., cold air drainage down mountainous slopes will affect DTR differently at the peak versus the foot of the mountains [61].

The different processes controlling DTR at different sites will inevitably affect the coefficient *b* and *c* of Bristow model. Detailed analysis of DTR on the TP and its possible effect on coefficients *b* and *c* will probably lead to a revised Bristow model suitable for regional application on the TP, but this is beyond the scope of this study.

In a word, the inhomogeneous distribution of the air mass, ozone and the content of pressure, together with the different processes influencing DTR caused by the special alpine climate conditions [55,60,62], contribute to the great variation in the coefficients of the empirical models on the TP and its surrounding regions.

3.2. Comparison of the Performance between Different Kinds of Methods

Comparison of the performance between the sunshine- and temperature-based models in Tables 1 and 2 indicates that the sunshine-based models outperform the temperature-based ones. This conclusion is in good agreement with other studies e.g., [30,36,37], and it was also validated by a case study in Gaize in the center part of the TP [38]. Recently, observation data collected at 98 stations worldwide were used for model evaluation, and the results reconfirmed again that the sunshine-based Ångström model performed better than the temperature-based ones [39]. As all of the coefficients in the average and geographical models were from the sunshine- or temperature-based site-dependent models, the sunshine-based average and geographical models can be expected to be superior to the corresponding temperature-based ones, which have been identified by the results in Tables 3 and 5.

An Ångström-type average model has been suggested for solar radiation estimation in Northeast Plain of China [44], which performs well with the average coefficients *a* and *b* of 0.215 and 0.518, respectively. This performance can be attributed to the small coefficient variation, which is attributed to small difference in elevation and the homogenous climate conditions in this plain area. However, things can be quite different on the TP and its surrounding regions, where the coefficients vary greatly. The great variation in the coefficients means it may not be proper to use an average value to represent all of different locations on the TP and its surrounding regions. This conclusion is supported by the results in Table 3, which indicates that the values of *NSE* at two stations drop below 0.60 by using the Ångström-type simple/statistical models. Li et al. [53] developed an Ångström-type statistical average model based on the dataset collected at 4 stations on the TP, and the result identified clearly that big errors occurred at one of the four selected stations. As for the temperature-based average models, the coefficients were influenced by a number of factors as discussed above. Statistically averaging the coefficients leads to *NSE* values at 9 out of 15 stations dropped below 0.60 (Table 3). Even worse, simply averaging the coefficients leads to an almost total failure in radiation estimation (Table 3).

As the average model cannot take into account the variation in coefficients at different stations, the geographical model was preferred for the regional application. Li et al. [50] developed a temperature-based geographical model for estimating the annual mean of daily solar irradiation in southwest regions of China, using data from five stations ranging from 259 m to 1074 m. Different geographical models were also developed for different solar radiation zones in China [49]. We re-examined the results of these geographical models, and found that both sunshine- and temperature-based geographical models perform well in the other regions of China, especially in the plain areas. However, these geographical models were simply based on the empirical relationship between the model coefficients and the geographical parameters without any physical foundation, which means that it might lead to the unacceptable predictions under extreme conditions. For an example, when the altitude is as high as 8844.43 m in the Mountain Everest, the value of the coefficient $(a + b)$ in the Ångström-type general model would be 1.02. This is surely ridiculous, as the value of $(a + b)$ can never be larger than 1.0 according to the physical meaning mentioned above. Therefore, the geographical model definitely cannot be applicable in estimation of the annual mean of daily solar irradiation on the TP.

Unlike the geographical models, the improved Ångström-type model was developed based on the leading factors accounting for variation in the coefficients rather than geographical parameters such as latitude and longitude. In this study, the improved Ångström-type model was established based on two fundamental factors, i.e., altitude and water vapor pressure. They are skillful in predicting the coefficients at different stations (Figure 4), making the improved Ångström-type model perform much better than the average and geographical models. The superior performance of the improved Ångström-type model can be attributed to the suitable expression of a and $(a + b)$. In the improved Ångström-type model, the coefficient b was expressed as a function of the water vapor pressure, and the sum of coefficients $(a + b)$ was described as a function of the altitude. The coefficient b reflects the transmission characteristic of the atmosphere [42], which is mainly influenced by water vapor content on the TP [63]. As the water vapor content changes greatly at different locations on the TP [56], introduction of water vapor pressure in coefficient b can significantly improve the applicability of the Ångström model at regional scale, which has already been identified by Wang et al. [64]. Our recent case study on the TP also identified the important role of the water vapor pressure in the Ångström model [38], with parameters different with those fitted in this study due to different data samples. The sum of coefficient $(a + b)$ represents the transmittance on a clear day, under which condition the air mass plays an important role on radiative transfer. Air mass above the station site [54] is strongly determined by the altitude under clear sky conditions, due to negligible aerosol pollutions on the TP [58]. Thus, altitude is the leading factor influencing the variation in coefficients at different stations on the TP, which means that description of $(a + b)$ as the function of altitude is reasonable and physical.

Evaluation of several empirical models by Liu et al. [40] also suggested that the altitude was one of the leading factors to account for variations in $(a + b)$ [40]. The logarithm function of altitude used on the TP in this study was preferred to the simple linear function of altitude in the plain region, mainly due to the higher elevation on the TP. In addition, similar to the model suggested by Liu et al. [40], a two-step procedure to predict the coefficients b and a was believed to enable accurate fitting of the coefficients for Ångström model, due to the constraint of the $(a + b)$ relationship [40].

As discussed above, all of the six sunshine- and temperature-based site-dependent models can accurately simulate the annual mean of daily solar irradiation at 15 stations, but the sunshine-based site-dependent models performed better than the temperature-based ones. As the coefficients of the models vary greatly among different stations, these site-dependent models can only be used to estimate the annual mean of daily solar irradiation locally at the corresponding stations, and cannot be used for the regional prediction. For regional application, the coefficients of the site-dependent models at 15 stations were simply or statistically averaged to represent the regional coefficients to simulate the annual mean of daily solar irradiation at different locations, but these kind of average models performed badly. Compared to the average models, geographical models performed better, but still not ideally. The improved Ångström-type model performed much better than both average and geographical models, and can be successfully applied at the regional scale on the TP, as the leading factors influencing the variations in coefficients at different locations have been taken into account deliberately.

3.3. Limitation of the Improved Ångström-Type Model

By using the two-step procedure and taking into account the leading factors to fit coefficients of Ångström model, the improved Ångström-type model outperforms both the average and geographical models. However, this model is based on some of the assumptions discussed above, which will inevitably confine its applicability under some conditions. One of the main limitation stems from the objectives of this research and the data used in this study. As we want to accurately estimate the annual mean of daily solar irradiation on the TP, the dataset used to develop the model was mainly collected on the TP and its surrounding regions, with all of the elevation higher than 1000 m. This may result in the incapacity of the model to accurately predict radiation at lower altitudes. It can be seen clearly that the sum of coefficient $(a + b)$ in the model would yield negative values when the altitude is less than 1.75 m. Thus, we strongly suggest that the improved Ångström-type model should not be used in the other regions with lower elevations, especially the plain regions with altitude less than

1000 m. Another main limitation is due to the assumption in the model development that the changes in aerosol concentration on the TP are negligible and thus the effect of aerosol on the coefficients was not considered. This assumption has been validated on the TP in general [58,63], but is obviously inappropriate for the large cities adjacent to the TP. Therefore, the improved Ångström-type model is also invalid for application in the surrounding large populous cities like Kunming and Guiyang, due to their serious pollution caused by rapid industrialization in recent decades [65]. Attempt was made to improve the applicability of the improved Ångström-type model by involving more datasets from other parts of China, together with a modifying factor of aerosol [66]. However, ironically, this attempt made the model inadequate for estimating the annual mean of daily solar irradiation on the TP, with only little success in improving the accuracy of the annual mean of daily solar irradiation prediction for large cities around the TP.

3.4. Spatial Distribution of the Annual Mean of Solar Irradiation on the Tibetan Plateau

According to the Ångström model, correct calculation of the extra-terrestrial radiation and reasonable estimation of the coefficients are the basic premises for accurate simulation of the spatial distribution of the annual mean of daily solar irradiation on the TP. However, the previous version of spatial distribution of the annual mean of daily solar irradiation on the TP [52] was based on the Bristow-type simple average model, which has been identified as an unsuitable method for radiation estimation on the TP, as discussed above.

In this study, most stations are located in the eastern part of the TP (Figure 7a), which makes detailed comparison between rasterized values and the corresponding measurements possible. The annual mean of daily solar irradiation was compared point by point with the corresponding values at the 14 radiation stations in Figure 7a. The results of the comparison indicate that the annual mean of daily solar irradiation estimated in Figure 8b agrees well with the corresponding measured values at each of the 14 radiation stations. Very few weather stations are located in the central and western parts of the TP, and there is only one radiation station (Shiquanhe) situated in the most western part of the TP. Fortunately, solar radiation was observed at a weather station located at central TP from 2001 to 2005 [38]. The annual mean of daily observation value is 21.0 MJ·m^{-2} in Gaize (32 30 N, 84 06 E, and, 4420 m a.s.l.), which is quite close to the rasterized value of 21.8 MJ·m^{-2} in this study. Based on the comparison made above, we can have confidence in the validation of the spatial pattern of solar radiation distribution on the TP rasterized in this study.

Although the spatial distribution of the annual mean of daily solar irradiation on the TP can be envisaged to be reliable, we must keep in mind that the rasterized annual mean of daily solar irradiation were obtained from the gridded sunshine percentage and water vapor pressure, which were interpolated by the ANUSPLIN method [67]. Ahead of application, the ANUSPLIN method was validated at eight meteorological stations on the TP, among which only one station is situated in the central TP and none are located in the western TP. The ANUSPLIN method is believed to be superior in interpolation of meteorological variables [68], but greatest uncertainty was found in poorly sampled areas [69], which is the common defect for all of the interpolation methods [45]. Recently, the ANUSPLIN method and several other interpolation methods were used to interpolate the gridded daily meteorological dataset over China [70], and the results indicated that data interpolated with different kinds of methods showed great uncertainty in regions with sparse stations, especially on the western TP. Therefore, it can be cautiously speculated that great uncertainty of interpolation may exist in the detailed distribution of the annual mean of solar irradiation in the central and western part of the TP, and further in situ investigations of the annual mean of daily solar irradiation in this vast unpopulated region are very urgent in the near future.

In addition, it must be kept in mind that the global solar radiation referred in this study means solar radiation at horizontal level without the screening effect of surrounding environments, just like those mentioned in all of the references cited in this work, e.g., [38,40,53], etc. This kind of radiation is comparable to the global radiation collected in the weather stations, which is measured at horizontal level without any sheltering. Actual radiation can be calculated by topography models based on DEM, with the horizontal level radiation as the first indispensable input variable. In other words, accurate simulation of the horizontal level radiation is the first essential step towards the reliable estimation of the actual radiation at given locations, which is beyond the topic of this study. We also noticed that the recent availability of data on the atmospheric constituents (every 3 h, approx. every 80 km) from Copernicus Atmosphere Monitoring Service will be useful for solar radiation estimation. The availability of time-series of solar radiation in cloud-free conditions (global, direct, diffuse) for the TP provided by the McClear model (see www.soda-is.com) and the details could be found in Lefèvre et al. [71]. This model could be considered in future researches.

4. Materials and Methods

4.1. Study Area and Data Collection

Situated in the Southwest China, the TP is the highest plateau over the world, featuring the tallest mountain Everest at 8844.43 m. The TP belongs to a special Plateau Alpine climate zone, with low temperatures, little precipitation and abundant sunshine [62].

There are about 2400 meteorological stations routinely observing meteorological conditions in China, but most of them are distributed in the east part of the country (Figure 9). Considering that there are very few radiation stations on the TP, the radiation stations in its surrounding regions were also included in this study, aiming to both increase the number of stations and identify the variation of coefficients. The study region defined as in Figure 9 is similar to those in previous studies [52,72]. For accurate estimation of radiation distribution on the TP, the database with 2400 stations archived in the National Meteorological Information Center (NMIC) of China Meteorological Administration (CMA) was employed. Distribution of the solar radiation stations and the routine weather stations is shown in Figure 9. Detailed information about the radiation stations is given in Table 7. A dataset combining the 15 solar radiation stations was first established, including daily solar irradiation, sunshine hours, water vapor pressure, maximum and minimum temperature for the period 1993–2010. Then another dataset was also established for the routine weather stations, including daily sunshine hours and water vapor pressure for the same period. Both datasets were screened similar to rules described by Persaud et al. [73], i.e., daily observations would be excluded from the datasets if (1) any of the observations were missing; and (2) the measured radiation/extra-terrestrial radiation or the actual sunshine hours/potential sunshine hours was greater than 1. The dataset of solar radiation was divided into two sub-datasets. One sub-dataset from 1993 to 2007 was used for model calibration, while the other from 2008 to 2010 was used for model evaluation. The Digital Elevation Model (DEM) data used for generating the gridded climate map was provided by the National Gometic Center of China (NGCC), with spatial resolution of 1 km $\times$ 1 km.

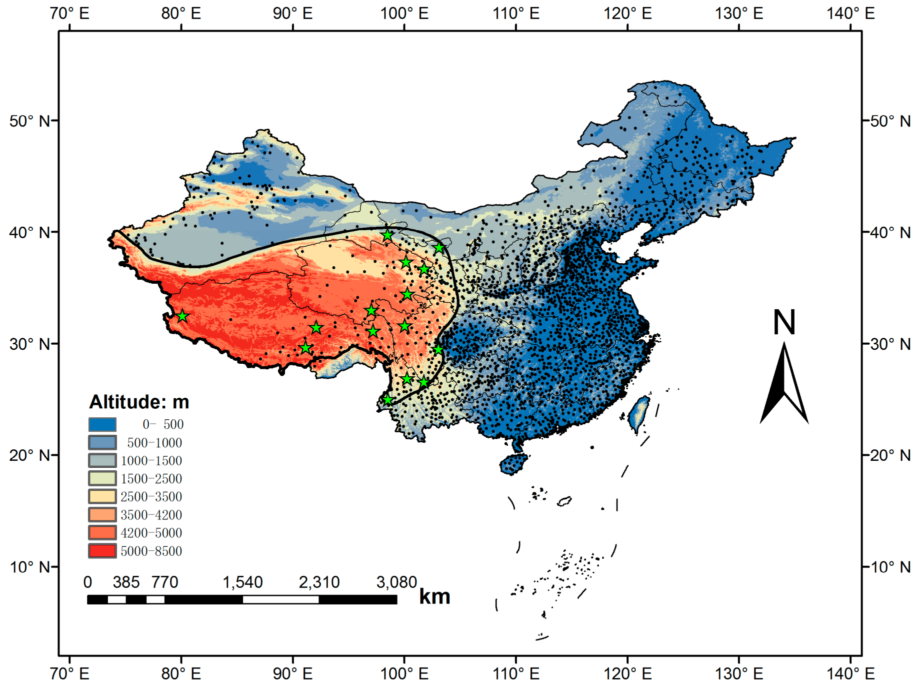

Figure 9. Distribution of solar radiation and weather stations. The black dots denote weather stations, and the five-point stars denote solar radiation stations used in this study.

Table 7. Detailed information of solar radiation stations in this study.

Station	Latitude/N°	Longitude/E°	Altitude/m asl
Jiuquan	39.77	98.48	1478.6
Minqin	38.63	103.08	1368.5
Gangcha	37.33	100.13	3302.4
Xining	36.72	101.75	2296.2
Shiquanhe	32.50	80.08	4279.3
Naqu	31.48	92.07	4808.0
Lhasa	29.67	91.13	3650.1
Yushu	33.02	97.02	3682.2
Guoluo	34.47	100.25	3720.5
Changdu	31.15	97.17	3307.1
Ganzi	31.62	100.00	3394.2
Ermeishan	29.52	103.33	3048.6
Lijiang	26.87	100.22	2393.9
Panzhihua	26.58	101.72	1191.1
Tengchong	25.02	98.50	1655.0

4.2. Model Description

In order to elucidate different methods for solar radiation estimation, four types of solar radiation models are defined and described as follows.

4.2.1. Site-Dependent Model

The coefficients of these models are site-dependent. Six site-dependent models, including three sunshine- and three temperature-based ones, were selected to evaluate their performances on the TP and its surrounding regions (Table 8).

Table 8. Selected models for estimating daily solar irradiation on the TP and its surrounding regions. H is ground solar irradiation ($MJ \cdot m^{-2}$), H_0 is the extra-terrestrial radiation ($MJ \cdot m^{-2}$), S is the actual sunshine hours (h), and S_0 is the potential sunshine hours (h). D is the temperature difference, which can be calculated as $D = T_m - [T_n(j) + T_n(j+1)]/2$, where T_m is daily maximum temperature (°C), $T_n(j)$ and $T_n(j+1)$ daily minimum temperature (°C) on the current and following days respectively. Parameters a, b, c and d are empirical coefficients. H_0 and S_0 can be calculated according to the procedure described by Allen et al. [9], and the coefficients can be fitted with numerical iteration methods [45].

Model Type	Model Name	Expression	Source
Sunshine-based	Angstrom	$H/H_0 = a + bS/S_0$	Angstrom et al. [23,24]
	Ogelman	$H/H_0 = a + b(S/S_0) + c(S/S_0)^2$	Ogelman et al. [25]
	Bahel	$H/H_0 = a + b(S/S_0) + c(S/S_0)^2 + d(S/S_0)^3$	Bahel et al. [26]
Temperature-based	Bristow	$H/H_0 = a(1 - \exp(bD^c))$	Bristow et al. [28]
	Hargreaves	$H/H_0 = a(T_m - T_n)^{0.5} + b$	Hargreaves et al. [29]
	Chen	$H/H_0 = a\ln(T_m - T_n) + b$	Chen et al. [30]

4.2.2. Average Model

In order to apply the site-dependent models regionally, two simple methods are suggested. One method is to obtain the regional coefficients by simply averaging coefficients from different radiation stations [45], which can be referred to as "simple-average model". Another method is to statistically fit the coefficients to a combined database from all the different radiation stations [44,52]. In the view of statistics [45], this method is referred to as "statistical-average model" hereinafter.

4.2.3. Geographical Model

Considering the regional variation in coefficients of the site-dependent models, some researchers tried to establish the relationship between model coefficients and geographical parameters, including latitude, longitude and altitude [30,49,50]. This is referred to as "geographical model" in this work.

4.2.4. Improved Ångström-Type Model

It is assumed that a numerical model based on the radiative transfer theory can be universally applied due to its robust mechanism [11,12]. However, its complex technique in model operation, together with the excessive requirements of input variables, makes it hard for practical application. Thus, models based on the relationship between coefficients and the leading factors accounting for coefficient variations were explored [40], which is referred to as "improved Ångström-type model" in this study.

4.3. Model Evaluation

The Nash-Sutcliffe Efficiency (NSE), the Mean Absolute Percentage Error ($MAPE$), and the Root Mean Squared Error ($RMSE$) [30,38,42,52], were used as criteria in evaluating the model performance in this study, and can be described as follows:

$$NSE = 1 - \frac{\sum_{i=1}^{n} (O_i - S_i)^2}{\sum_{i=1}^{n} (O_i - \overline{O})^2} \tag{4}$$

$$MAPE = \frac{\sum_{i=1}^{n} \frac{|O_i - S_i|}{O_i} \times 100}{n} \tag{5}$$

$$RMSE = [\frac{1}{n}\sum_{i=1}^{n}(O_i - S_i)^2]^{\frac{1}{2}} \quad (6)$$

where O_i is the observed value, S_i is the simulated value, $\overline{O}$ is the average value of the observed radiation, and n is the number of observations. Since *MAPE* is expressed as percentage whereas *RMSE* does not, *RRMSE* is used in place of *RMSE* for comparison with *MAPE*. *RRMSE* is the ration of *RMSE* to the average value of the observation, which is also expressed as percentage [74]. The greater the *NSE* and the lower the *MAPE* and *RRMSE*, the better the model. Slope and Inter are the slope and intercept of the linear regression between observed and simulated, respectively. The t-test was used to identify significant differences between the results of the selected models [75,76], and the value of t was calculated as [36,40]:

$$t = \sqrt{\frac{(n-1)\times MBE^2}{(RMSE^2 - MBE^2)}} \quad (7)$$

where MBE was the bias [38,42]:

$$MBE = \frac{1}{n}\sum_{i=1}^{n}(S_i - O_i) \quad (8)$$

When the calculated $|t| \geq t_{0.05}$ (critical value), the two groups of data are considered to differ significantly.

4.4. Australia National University SPLINe (ANUSPLIN) Interpolation Method

The ANUSPLIN (version 4.3, Australia National University, Canberra, Australia) was used to spatially interpolate sunshine hours and water vapor pressure in this study, based on which the distribution of the annual mean of daily solar irradiation was rasterized. The ANUSPLIN was developed by the Australian National University in order to provide a facility for transparent analysis and interpolation of noisy multivariate data using thin plate smoothing splines [67]. Given its full consideration of the effect of latitude, longitude and altitude on meteorological interpolation, the method has been more popular than other interpolation methods [68], and a detailed description of ANUSPLIN can be referred in [67–69].

5. Conclusions

This study investigated the performance of different site-dependent models based on 15 radiation stations in the TP and its surrounding regions. We found that the coefficients varied greatly among different site-dependent models over the TP, due to the great spatial difference in elevation, water vapor content, complex terrain and also the climate characteristics. The sunshine-based models have better simulation accuracy than temperature-based ones for radiation estimation locally. The simple and statistical average Ångström-based models perform poorly at several stations. The Bristow-based simple/statistical average models perform even worse at most of the stations. Geographical Ångström-type models perform much better than the average models, but it might lead to unacceptable predictions under extreme conditions, as its coefficients are simply fitted by the geographical parameters without any physical foundation.

In order to achieve better performance for estimating solar radiation over the TP, a simple improved Ångström-type model was established using altitude and water vapor pressure as the leading factors accounting for the great variations in the coefficients. The improved model reproduced the coefficients quite well, and has the best performance among all models. Spatial distribution of solar radiation on the TP was then estimated based on the improved Ångström-type model and ANUSPLIN method. The overall pattern of radiation distribution was validated point by point at the 15 solar radiation stations. The estimation showed that solar radiation increases from east to west. Solar radiation in southwest TP is the greatest. Solar radiation estimation results for the TP based on the new model including the coefficients and rasterized solar radiation are available upon request.

Acknowledgments: This research is jointly supported by Special Fund for Meteorology Research in China (GYHY201306048 & GYHY201106024) and the Key Project on the Second Exploration of Meteorological and Energy Conditions on the Tibetan Plateau, and also the National Natural Science Foundation of China (41671107 & 41301092). Deliang Chen is supported by a grant from the Swedish Research Council. We authors are grateful to National Meteorological Information Center for the authorization of access to the full database in this study. Special thank is also due to the weathermen working hard on the Tibetan Plateau under altitude hypoxia conditions.

Author Contributions: Tao Pan and Jiandong Liu conceived and designed the experiments; Jiandong Liu performed the experiments; Jiandong Liu and Tao Pan analyzed the data; Deliang Chen, Xiuji Zhou, Qiang Yu, Gerald N. Flerchinger, De Li Liu, Xintong Zou, Hans W. Linderholm, Jun Du, Dingrong Wu and Yanbo Shen contributed data/materials/analysis methods and discussion; Jiandong Liu wrote the paper.

Conflicts of Interest: The authors declare no conflict of interest.

References

1. Yaghoubi, M.A.; Sabzevari, A. Further data on solar radiation in Shiraz, Iran. *Renew. Energy* **1996**, *7*, 393–399. [CrossRef]
2. Colak, I.; Sagiroglu, S.; Demirtas, M.; Yesilbudak, M. A data mining approach: Analyzing wind speed and insolation period data in Turkey for installations of wind and solar power plants. *Energy Convers. Manag.* **2013**, *65*, 185–197. [CrossRef]
3. Wong, L.T.; Chow, W.K. Solar radiation model. *Appl. Energy* **2001**, *69*, 191–224. [CrossRef]
4. Yue, C.D.; Huang, G.R. An evaluation of domestic solar energy potential in Taiwan incorporating land use analysis. *Energy Policy* **2011**, *39*, 7988–8002. [CrossRef]
5. Abraha, M.G.; Savage, M.J. Comparison of estimates of daily solar radiation from air temperature range for application in crop simulations. *Agric. For. Meteorol.* **2008**, *148*, 401–416. [CrossRef]
6. Hunt, L.A.; Kuchar, L.S.; Swanton, C.J. Estimation of solar radiation for use in crop modeling. *Agric. For. Meteorol.* **1998**, *91*, 293–300. [CrossRef]
7. Cristea, N.C.; Kampf, S.K.; Burges, S.J. Linear models for estimating annual and growing season reference evapotranspiration using averages of weather variables. *Int. J. Climatol.* **2013**, *33*, 376–387. [CrossRef]
8. Kang, M.S.; Park, S.W.; Lee, J.J.; Yoo, K.H. Applying SWAT for TMDL programs to a small watershed containing rice paddy fields. *Agric. Water Manag.* **2006**, *79*, 72–92. [CrossRef]
9. Allen, R.G.; Pereira, L.S.; Raes, D.; Smith, M. *Crop Evapotranspiration-Guidelines for Computing Crop Water Requirements*; FAO Irrigation and Drainage Paper 56; Food and Agriculture Organization of the United Nations: Rome, Italy, 1998; Volume 300, p. D05109.
10. Weiss, A.; Hays, C.J. Simulation of daily solar irradiance. *Agric. For. Meteorol.* **2004**, *123*, 187–199. [CrossRef]
11. Morcrette, J.J.; Mozdzynski, G.; Leutbecher, M. A reduced radiation grid for the ECMWF integrated forecasting system. *Mon. Weather Rev.* **2008**, *136*, 4760–4772. [CrossRef]
12. Manners, J.; Thelen, J.C.; Petch, J.; Hill, P.; Edwards, J.M. Two fast radiative transfer methods to improve the temporal sampling of clouds in numerical weather prediction and climate models. *Q. J. R. Meteorol. Soc.* **2009**, *135*, 457–468. [CrossRef]
13. Tymvios, F.S.; Jacovides, C.P.; Michaelides, S.C.; Scouteli, C. Comparative study of Angstrom's and artificial neural network's methodologies in estimating global solar radiation. *Sol. Energy* **2005**, *70*, 752–762. [CrossRef]
14. Jacovides, C.P.; Tymvios, F.S.; Boland, J.; Tsitouri, M. Artificial Neural Network models for estimating daily solar global UV, PAR and broadband radiant fluxes in an eastern Mediterranean site. *Atmos. Res.* **2015**, *152*, 138–145. [CrossRef]
15. Fadare, D.A. Modelling of solar energy potential in Nigeria using an artificial neural network model. *Appl. Energy* **2009**, *86*, 1410–1422. [CrossRef]
16. Şenkal, O.; Kuleli, T. Estimation of solar radiation over Turkey using artificial neural network and satellite data. *Appl. Energy* **2009**, *86*, 1222–1228. [CrossRef]
17. Mihalakakou, G.; Santamouris, M.; Asimakopoulos, D.N. The total solar radiation time series simulation in Athens, using neural networks. *Theor. Appl. Climatol.* **2000**, *66*, 185–197. [CrossRef]
18. Qin, J.; Chen, Z.; Yang, K.; Liang, S.; Tang, W. Estimation of monthly-mean daily global solar radiation based on MODIS and TRMM products. *Appl. Energy* **2011**, *88*, 2480–2489. [CrossRef]
19. Janjai, S.; Pankaew, P.; Laksanaboonsong, J. A model for calculating hourly global solar radiation from satellite data in the tropics. *Appl. Energy* **2009**, *86*, 1450–1457. [CrossRef]

20. Hinkelman, L.M.; Stackhouse, P.W., Jr.; Wielicki, B.A.; Zhang, T.; Wilson, S.R. Surface insolation trends from satellite and ground measurements: Comparisons and challenges. *J. Geophys. Res. Atmos.* **2009**, *114*, 4427–4433. [CrossRef]
21. Pinker, R.T.; Frouin, R.; Li, Z. A review of satellite methods to derive surface shortwave irradiance. *Remote Sens. Environ.* **1995**, *51*, 108–124. [CrossRef]
22. Boilley, A.; Wald, L. Comparison between meteorological re-analyses from ERA-Interim and MERRA and measurements of daily solar irradiation at surface. *Renew. Energy* **2015**, *75*, 135–143. [CrossRef]
23. Ångström, A. Solar and terrestrial radiation. *Q. J. R. Met. Soc.* **1924**, *50*, 121–125.
24. Prescott, J. Evaporation from a water surface in relation to solar radiation. *Trans. R. Soc. S. Aust.* **1940**, *64*, 114–118.
25. Ögelman, H.; Ecevit, A.; Tasdemiroğlu, E. A new method for estimating solar radiation from bright sunshine data. *Sol. Energy* **1984**, *33*, 619–625. [CrossRef]
26. Bahel, V.; Bakhsh, H.; Srinivasan, R. A correlation for estimation of global solar radiation. *Energy* **1987**, *12*, 131–135. [CrossRef]
27. Ampratwum, D.B.; Dorvlo, A.S.S. Estimation of solar radiation from the number of sunshine hours. *Appl. Energy* **1999**, *63*, 161–167. [CrossRef]
28. Bristow, K.L.; Campbell, G.S. On the relationship between incoming solar radiation and daily maximum and minimum temperature. *Agric. For. Meteorol.* **1984**, *31*, 159–166. [CrossRef]
29. Hargreaves, G.L.; Hargreaves, G.H.; Riley, J.P. Irrigation water requirements for Senegal River Basin. *J. Irrig. Drain. Eng.* **1985**, *111*, 265–275. [CrossRef]
30. Chen, R.; Kang, E.; Yang, J.; Lu, S.; Zhao, W. Validation of five global radiation models with measured daily data in China. *Energy Convers. Manag.* **2004**, *45*, 1759–1769. [CrossRef]
31. Meza, F.; Varas, E. Estimation of mean monthly solar global radiation as a function of temperature. *Agric. For. Meteorol.* **2000**, *100*, 231–241. [CrossRef]
32. Goodin, D.G.; Hutchinson, J.M.S.; Vanderlip, R.L.; Knapp, M.C. Estimating solar irradiance for crop modeling using daily air temperature data. *Agron. J.* **1999**, *91*, 845–851. [CrossRef]
33. Weiss, A.; Hays, C.J.; Hu, Q.; Easterling, W.E. Incorporating bias error in calculating solar irradiance: Implications for crop yield simulations. *Agron. J.* **2001**, *93*, 1321–1326. [CrossRef]
34. Liu, D.L.; Scott, B.J. Estimation of solar radiation in Australia from rainfall and temperature observations. *Agric. For. Meteorol.* **2001**, *106*, 41–59. [CrossRef]
35. Mccaskill, M.R. Prediction of solar radiation from rainday information using regionally stable coefficients. *Agric. For. Meteorol.* **1990**, *51*, 247–255. [CrossRef]
36. Wu, G.; Liu, Y.; Wang, T. Methods and strategy for modeling daily global solar radiation with measured meteorological data—A case study in Nanchang station, China. *Energy Convers. Manag.* **2007**, *48*, 2447–2452. [CrossRef]
37. Podestá, G.P.; Núñez, L.; Villanueva, C.A.; Skansi, M.A.A. Estimating daily solar radiation in the Argentine Pampas. *Agric. For. Meteorol.* **2004**, *123*, 41–53. [CrossRef]
38. Liu, J.; Liu, J.; Linderholm, H.W.; Chen, D.; Yu, Q.; Wu, D.; Haginoya, S. Observation and calculation of the solar radiation on the Tibetan Plateau. *Energy Convers. Manag.* **2012**, *57*, 23–32. [CrossRef]
39. Moradi, I.; Mueller, R.; Perez, R. Retrieving daily global solar radiation from routine climate variables. *Theor. Appl. Climatol.* **2014**, *116*, 661–669. [CrossRef]
40. Liu, X.; Xu, Y.; Zhong, X.; Zhang, W.; Porter, J.R.; Liu, W. Assessing models for parameters of the Ångström-Prescott formula in China. *Appl. Energy* **2012**, 327–338. [CrossRef]
41. Liu, X.; Mei, X.; Li, Y.; Wang, Q.; Jensraunsø, J.; Zhang, Y.; Johnroy, P. Evaluation of temperature-based global solar radiation models in China. *Agric. For. Meteorol.* **2009**, *149*, 1433–1446. [CrossRef]
42. Liu, X.; Mei, X.; Li, Y.; Porter, J.R.; Wang, Q.; Zhang, Y. Choice of the Ångström–Prescott coefficients: Are time-dependent ones better than fixed ones in modeling global solar irradiance? *Energy Convers. Manag.* **2010**, *51*, 2565–2574. [CrossRef]
43. Wu, D.; Qiang, Y.; Lu, C.; Hengsdijk, H. Quantifying production potentials of winter wheat in the North China Plain. *Eur. J. Agron.* **2006**, *24*, 226–235. [CrossRef]
44. Wu, Z.; Du, H.; Zhao, D.; Ming, L. Estimating daily global solar radiation during the growing season in Northeast China using the Ångström–Prescott model. *Theor. Appl. Climatol.* **2012**, *108*, 495–503. [CrossRef]

45. Von Storch, H.; Zwiers, F.W. *Statistical Analysis in Climate Research*; Cambridge University Press: Cambridge, UK, 2001; pp. 3–10.
46. Chen, R.; Lu, S.; Kang, E.; Yang, J.; Ji, X. Estimating daily global radiation using two types of revised models in China. *Energy Convers. Manag.* **2006**, *47*, 865–878.
47. Zhou, J.; Wu, Y.; Gang, Y. General formula for estimation of monthly average daily global solar radiation in China. *Energy Convers. Manag.* **2005**, *46*, 257–268.
48. Wu, W.; Liu, H.B. Assessment of monthly solar radiation estimates using support vector machines and air temperatures. *Int. J. Climatol.* **2012**, *32*, 274–285. [CrossRef]
49. Li, M.F.; Tang, X.P.; Wu, W.; Liu, H.B. General models for estimating daily global solar radiation for different solar radiation zones in Mainland China. *Energy Convers. Manag.* **2013**, *70*, 139–148. [CrossRef]
50. Li, M.F.; Fan, L.; Liu, H.B.; Guo, P.T.; Wu, W. A general model for estimation of daily global solar radiation using air temperatures and site geographic parameters in Southwest China. *J. Atmos. Sol. Terr. Phys.* **2013**, *92*, 145–150. [CrossRef]
51. Wang, Q.; Qiu, H.N. Situation and outlook of solar energy utilization in Tibet, China. *Renew. Sustain. Energy Rev.* **2009**, *13*, 2181–2186. [CrossRef]
52. Pan, T.; Wu, S.; Dai, E.; Liu, Y. Estimating the daily global solar radiation spatial distribution from diurnal temperature ranges over the Tibetan Plateau in China. *Appl. Energy* **2013**, *107*, 384–393. [CrossRef]
53. Li, H.; Ma, W.; Lian, Y.; Wang, X.; Zhao, L. Global solar radiation estimation with sunshine duration in Tibet, China. *Renew. Energy* **2011**, *36*, 3141–3145. [CrossRef]
54. Liou, K. *An introduction to Atmospheric Radiation*, 2nd ed.; Elsevier Science: San Diego, CA, USA, 2002.
55. Dai, J. *The Climate over the Tibetan Plateau*; Meteorological Press: Beijing, China, 1990. (In Chinese)
56. Liu, J.; Sun, Z.; Liang, H.; Xu, X.; Wu, P. Precipitable water vapor on the Tibetan Plateau estimated by GPS, water vapor radiometer, radiosonde, and numerical weather prediction analysis and its impact on the radiation budget. *J. Geophys. Res. Atmos.* **2005**, *110*. [CrossRef]
57. Yang, K.; Huang, G.W.; Tamai, N. A hybrid model for estimating global solar radiation. *Sol. Energy* **2001**, *70*, 13–22. [CrossRef]
58. Streets, D.G.; Yu, C.; Wu, Y.; Chin, M.; Zhao, Z.; Hayasaka, T.; Shi, G. Aerosol trends over China, 1980–2000. *Atmos. Res.* **2008**, *88*, 174–182. [CrossRef]
59. Zhou, X.; Luo, C. Ozone valley over Tibetan Plateau. *Acta Meteorol. Sin.* **1994**, *8*, 505–506.
60. Yu, Q.; Liu, Y.; Liu, J.; Wang, T. Simulation of leaf photosynthesis of winter wheat on Tibetan Plateau and in North China plain. *Ecol. Model.* **2002**, *155*, 205–216. [CrossRef]
61. Arya, S. *Introduction to Micrometeorology*; Academic Press: San Diego, CA, USA, 2001.
62. Domrös, M.; Peng, G. *The Climate of China*; Springer: Berlin/Heidelberg, Germany, 1988; pp. 258–278.
63. Yang, K.; Ding, B.; Qin, J.; Tang, W.; Lu, N.; Lin, C. Can aerosol loading explain the solar dimming over the Tibetan Plateau? *Geophys. Res. Lett.* **2012**, *39*. [CrossRef]
64. Wang, B.; Zhang, G.; Li, L. *Thesis on Wind and Solar Energy in China*; Meteorological Press: Beijing, China, 2008. (In Chinese)
65. Wang, Y.; Yang, Y.; Han, S.; Wang, Q.; Zhang, J. Sunshine dimming and brightening in Chinese cities (1955–2011) was driven by air pollution rather than clouds. *Clim. Res.* **2013**, *56*, 11–20. [CrossRef]
66. Zhao, N.; Zeng, X.; Han, S. Solar radiation estimation using sunshine hour and air pollution index in China. *Energy Convers. Manag.* **2013**, *76*, 846–851. [CrossRef]
67. Hutchinson, M.F. *ANUSPLIN Version 4.36 User Guide*; The Australia Nationaluniversity, Center for Resource and Environment Studies: Canberra, Australia, 2006.
68. Price, D.T.; Mckenney, D.W.; Nalder, I.A.; Hutchinson, M.F.; Kesteven, J.L. A comparison of two statistical methods for spatial interpolation of Canadian monthly mean climate data. *Agric. For. Meteorol.* **2000**, *101*, 81–94. [CrossRef]
69. Hijmans, R.J.; Cameron, S.E.; Parra, J.L.; Jones, P.G.; Jarvis, A. Very high resolution interpolated climate surfaces for global land areas. *Int. J. Climatol.* **2005**, *25*, 1965–1978. [CrossRef]
70. Wu, J.; Gao, X. A gridded daily observation dataset over China region and comparison with the other datasets. *Chin. J. Geophys.* **2013**, *56*, 1102–1111. (In Chinese)
71. Lefèvre, M.; Oumbe, A.; Blanc, P.; Espinar, B.; Gschwind, B.; Qu, Z.; Wald, L.; Schroedter-Homscheidt, M.; Hoyer-Klick, C.; Arola, A.; et al. McClear: A new model estimating downwelling solar radiation at ground level in clear-sky condition. *Atmos. Meas. Tech.* **2013**, *6*, 2403–2418. [CrossRef]

72. Zhang, Y.; Liu, C.; Tang, Y.; Yang, Y. Trends in pan evaporation and reference and actual evapotranspiration across the Tibetan Plateau. *J. Geophys. Res. Atmos.* **2007**, *112*, 113–120. [CrossRef]
73. Persaud, N.; Lesolle, D.; Ouattara, M. Coefficients of the Ångström-Prescott equation for estimating global irradiance from hours of bright sunshine in Botswana and Niger. *Agric. For. Meteorol.* **1997**, *88*, 27–35. [CrossRef]
74. Willmott, C.T.; Matsuura, K. Advantages of the mean absolute error (MAE) over the root mean square error (RMSE) in assessing average model performance. *Clim. Res.* **2005**, *30*, 79–82. [CrossRef]
75. Stone, R.J. Improved statistical procedure for the evaluation of solar radiation estimation models. *Sol. Energy* **1993**, *51*, 289–291. [CrossRef]
76. Jacovides, C.P.; Kontoyiannis, H. Statistical procedures for the evaluation of evapotranspiration computing models. *Agric. Water Manag.* **1995**, *27*, 365–371. [CrossRef]